A Linear Hybrid-Variable Approach for Advection Equations

Xianyi Zeng

Department of Mathematical Sciences
University of Texas at El Paso, El Paso, TX.

Computational Science Graduate Seminar
University of Texas at El Paso
El Paso, TX. April 16th, 2018

Outline

The Advection Equation

The Cauchy problem of the advection equation

$$\begin{cases} w_t + c\, w_x = 0\,, & (x,t) \in [0,\ L] \times \mathbb{R}^+ \\ w(0,t) = w(L,t)\,, & t \in \mathbb{R}^+ \\ w(x,0) = w_{\text{init}}(x)\,, & x \in [0,\ L]\,. \end{cases}$$

Exact solution is simple and well-known

$$w(x,t) = w_{\text{init}}(x - ct)\,.$$

The Advection Equation

The Cauchy problem of the advection equation

$$\begin{cases} w_t + c\, w_x = 0\ , & (x,t) \in [0,\ L] \times \mathbb{R}^+ \\ w(0,t) = w(L,t)\ , & t \in \mathbb{R}^+ \\ w(x,0) = w_{\text{init}}(x)\ , & x \in [0,\ L]\ . \end{cases}$$

Exact solution is simple and well-known

$$w(x,t) = w_{\text{init}}(x - ct)\ .$$

Numerical methods, however

- Finite difference methods (MacCormack, JST, WENO, ...).
- Finite volume methods (Flux Splitting, MUSCL, K-Exact, ...).
- Petrov-Galerkin finite element methods (SUPG, VMS, ...).
- Discontinuous Galerkin methods (RKDG, HDG, ...).
- Spectral methods (SDM, SEM, ...).
- And their variants...

The Advection Equation

The Cauchy problem of the advection equation

$$\begin{cases} w_t + c\, w_x = 0\ , & (x,t) \in [0,\ L] \times \mathbb{R}^+ \\ w(0,t) = w(L,t)\ , & t \in \mathbb{R}^+ \\ w(x,0) = w_{\text{init}}(x)\ , & x \in [0,\ L]\ . \end{cases}$$

Exact solution is simple and well-known

$$w(x,t) = w_{\text{init}}(x - ct)\ .$$

Numerical methods, however

- Finite difference methods (MacCormack, JST, WENO, ...).
- Finite volume methods (Flux Splitting, MUSCL, K-Exact, ...).
- Petrov-Galerkin finite element methods (SUPG, VMS, ...).
- Discontinuous Galerkin methods (RKDG, HDG, ...).
- Spectral methods (SDM, SEM, ...).
- And their variants...

Finite-Difference and Finite-Volume Discretizations

Finite difference methods

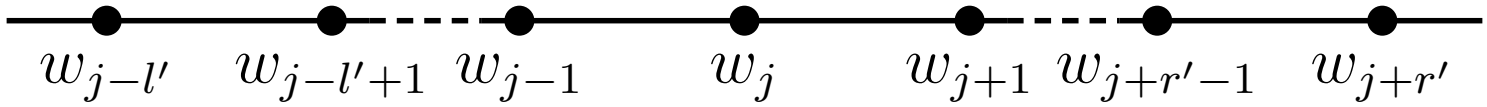

- Approximations to nodal solutions:

$$w_j(t) \approx w(x_j\ ,t)\ , \quad w_j^n \approx w(x_j\ ,t^n)\ .$$

- Semi-discretization in space:

$$\frac{dw_j}{dt} + c\mathcal{D}_x w_j = 0\ .$$

- Discrete differential operator (DDO):

$$\mathcal{D}_x w_j = \frac{1}{h}\left(\beta_{-l'} w_{j-l'} + \cdots + \beta_0 w_j + \cdots + \beta_{r'} w_{j+r'}\right)$$

Finite-Difference and Finite-Volume Discretizations

Finite volume methods

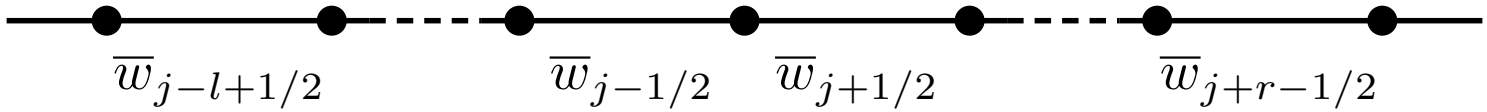

- Approximations to cell-averaged solutions:

$$\overline{w}_{j+1/2}(t) \approx \frac{1}{h}\int_{x_j}^{x_{j+1}} w(x\ ,t)dx\ , \quad \overline{w}^n_{j+1/2} \approx \frac{1}{h}\int_{x_j}^{x_{j+1}} w(x\ ,t^n)dx\ .$$

- Semi-discretization in space:

$$\frac{d\overline{w}_{j+1/2}}{dt} + \frac{1}{h}\left(\mathcal{F}_{j+1} - \mathcal{F}_j\right) = 0\ .$$

- Numerical flux:

$$\mathcal{F}_j = \mathcal{F}(\overline{w}_{j-l+1/2}, \cdots, \overline{w}_{j+r-1/2})\ .$$

The Hybrid-Variable Approach

Discretization with both cell-averages and nodal values

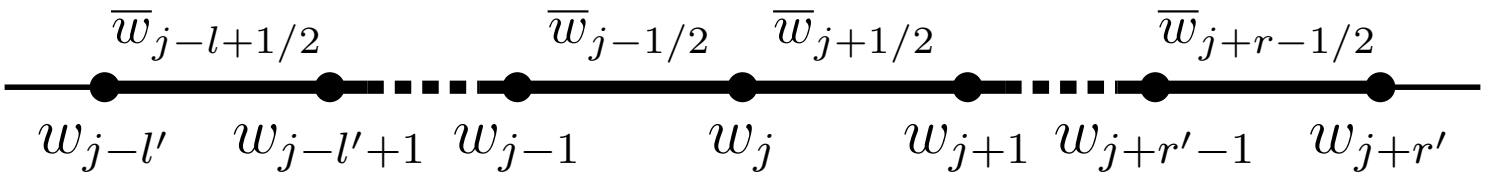

- Conservative updates for cell-averages:

$$\frac{d\overline{w}_{j+1/2}}{dt} + \frac{1}{h}\left(cw_{j+1} - cw_j\right) = 0 \ .$$

- Discretizing the strong form of the equation for nodal values:

$$\frac{dw_j}{dt} + c[\mathcal{D}_x w]_j = 0 \ .$$

- The hybrid-variable discrete differential operator:

$$[\mathcal{D}_x w]_j = \frac{1}{h}\sum_{k=-l}^{r-1} \alpha_k \overline{w}_{j+k+1/2} + \frac{1}{h}\sum_{k=-l'}^{r'} \beta_k w_{j+k} \ .$$

The Hybrid-Variable Approach

Discretization with both cell-averages and nodal values

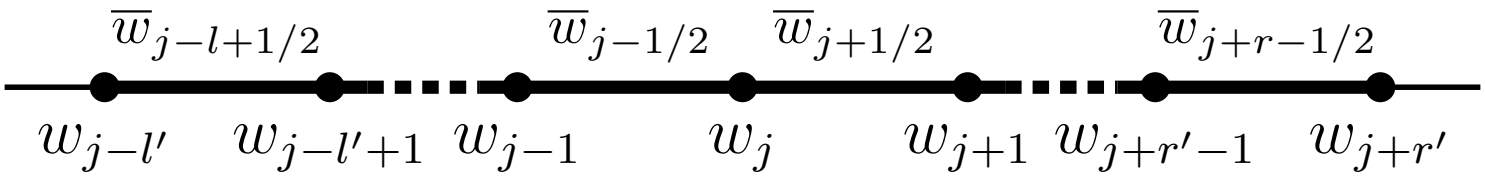

- Fundamental questions to answer:
  - How well does $[\mathcal{D}_x w]_j$ approximate $w_x(x_j, t)$?
  - Does the operator $[\mathcal{D}_x w]_j$ exists?
  - How accurate are the HV methods?
  - Are they stable?

General HV-DDO with Compact Stencils

HV-DDO with compact stencils

- Case 1: $l' = l,\ r' = r.$

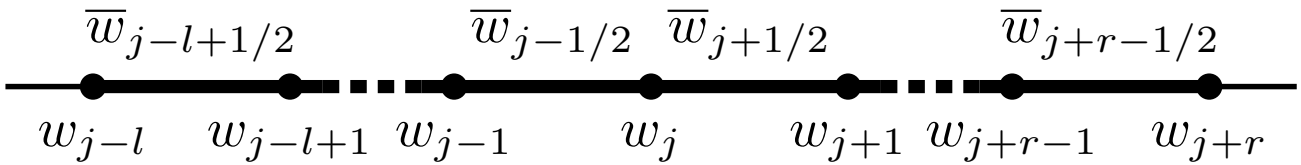

- Case 2: $l' = l - 1,\ r' = r.$

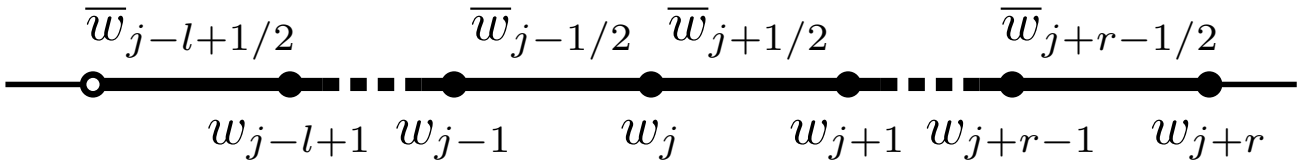

- Case 3: $l' = l,\ r' = r - 1.$

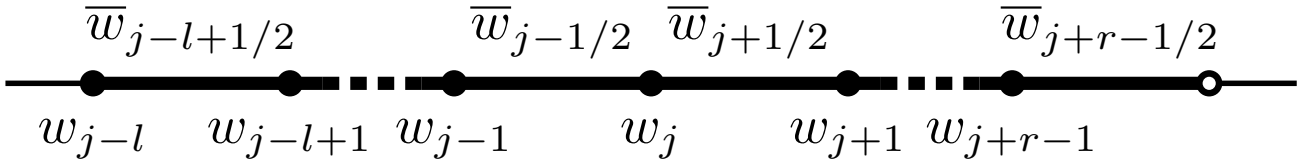

- Case 4: $l' = l - 1,\ r' = r - 1.$

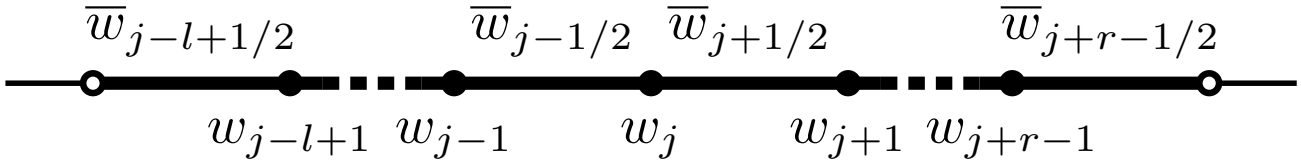

General HV-DDO with Compact Stencils

Constructing a high-order HV-DDO

Definition

The operator $[\mathcal{D}_x]$ is p^{th}-order accurate if for any C^∞ function $w(x)$:

$$[\mathcal{D}_x w]_j = \partial_x w(x_j) + c_p \partial_x^{p+1} w(x_j) h^p + O(h^{p+1}) \ ,$$

for some $c_p \neq 0$, where the exact data is used to evaluate the left hand side.

Example:

$$\begin{aligned}\overline{w}_{j-1/2} &= \frac{1}{h}\int_{x_{j-1}}^{x_j} w(x)dx = \frac{1}{h}\int_0^h \left(w_j - s\partial_x w_j + \frac{1}{2}s^2\partial_x^2 w_j + O(h^3) \right) ds \\ &= w_j - \frac{1}{2}h\partial_x w_j + \frac{1}{6}h^2\partial_x^2 w_j + O(h^3) \ .\end{aligned}$$

Thus $[\mathcal{D}_x w]_j = 2(w_j - \overline{w}_{j-1/2})/h$ is a 1^{st}-order HV-DDO.

Case 1: HV-DDO and Balanced Hermite Interpolation

Existence of HV-DDO – Case 1: $l' = l$ and $r' = r$.

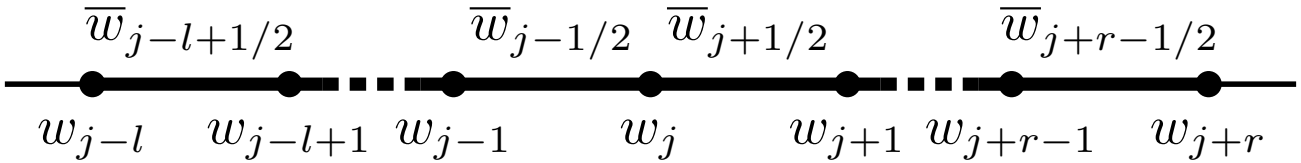

p-exactness of HV-DDO:

- $[\mathcal{D}_x w]_j$ is at least p^{th}-order accurate if for all $q(x) \in \mathbb{P}^p$

$$[\mathcal{D}_x q]_j = q'(x_j) \, .$$

- Let $Q(x) = \int_0^x q(y)dy \in \mathbb{P}^{p+1}$, p-exactness indicates:

$$Q''(x_j) = \frac{1}{h^2} \sum_{k=-l}^{r-1} \alpha_k (Q(x_{j+k+1}) - Q(x_{j+k})) + \frac{1}{h} \sum_{k=-l'}^{r'} \beta_k Q'(x_{j+k}) \, .$$

- Hermite interpolation with one derivative at $r + l + 1$ grid points: $x_{j-l}, \cdots, x_j, \cdots, x_{j+r}$!

Case 1: HV-DDO and Balanced Hermite Interpolation

Relation to balanced Hermite Interpolation

- Any $Q \in \mathbb{P}^{2(l+r)+1}$ can be written uniquely as:

$$Q(x) = \sum_{-l \le k \le r} Q(x_{j+k}) h_k(x) + \sum_{-l \le k \le r} Q'(x_{j+k}) g_k(x) \ .$$

- $h_k(x)$ and $g_k(x)$ are fundamental polynomials for the first and second kind for balanced Hermite interpolations.
- Setting $x = x_j$ and matching the coefficients:

$$\Delta\alpha_k = \alpha_k - \alpha_{k-1} = h^2 h_k''(x_j) \ , \quad -l \le k \le r \ ,$$
$$\beta_k = h g_k''(x_j) \ , \quad -l \le k \le r \ .$$

Lemma

When $r' = r$ and $l' = l$, there exists a unique HV-DDO that is at least $2(l+r)^{\text{th}}$-order accurate.

HV-DDO with Arbitrary Order of Accuracy

Optimal order of HV-DDO with compact stencil

Theorem

There exists a unique $[\mathcal{D}_x]$ with order of accuracy $l+r+l'+r'$, whose coefficients are given by:

$$\alpha_\nu = \delta_{ll'}\frac{2}{l^2}C_{-l}^{l,r}C_{-l}^{l,r'} + \sum_{k=-l'}^{\nu}\frac{2(1+k(\zeta_k^{l,r}+\zeta_k^{l',r'}))}{k^2}C_k^{l,r}C_k^{l',r'}\ ,\quad \forall -l\le\nu<0\ ,$$

$$\alpha_\nu = -\sum_{k=\nu+1}^{r'}\frac{2(1+k(\zeta_k^{l,r}+\zeta_k^{l',r'}))}{k^2}C_k^{l,r}C_k^{l',r'} - \delta_{rr'}\frac{2}{r^2}C_r^{l,r}C_r^{l',r}\ ,\quad \forall 0\le\nu\le r-1\ ;$$

$$\beta_0 = 2(\zeta_0^{l,r}+\zeta_0^{l',r'})\ ,$$

$$\beta_\nu = -\frac{2}{\nu}C_\nu^{l,r}C_\nu^{l',r'}\ ,\quad -l'\le\nu\le r',\quad \nu\neq 0\ .$$

- Construct the fundamental interpolation polynomials for unbalanced Hermite interpolation in the other three cases.
- Explictly compute the coefficients α_k and β_k.
- Show $c_p\neq 0$ for $p=l+r+l'+r'$.

HV-DDO with Arbitrary Order of Accuracy

Optimal order of HV-DDO with compact stencil

Theorem

There exists a unique $[\mathcal{D}_x]$ with order of accuracy $l+r+l'+r'$, whose coefficients are given by:

$$\alpha_\nu = \delta_{ll'}\frac{2}{l^2}C_{-l}^{l,r}C_{-l}^{l,r'} + \sum_{k=-l'}^{\nu}\frac{2(1+k(\zeta_k^{l,r}+\zeta_k^{l',r'}))}{k^2}C_k^{l,r}C_k^{l',r'}\ ,\quad \forall -l\le\nu<0\ ,$$

$$\alpha_\nu = -\sum_{k=\nu+1}^{r'}\frac{2(1+k(\zeta_k^{l,r}+\zeta_k^{l',r'}))}{k^2}C_k^{l,r}C_k^{l',r'} - \delta_{rr'}\frac{2}{r^2}C_r^{l,r}C_r^{l',r}\ ,\quad \forall 0\le\nu\le r-1\ ;$$

$$\beta_0 = 2(\zeta_0^{l,r}+\zeta_0^{l',r'})\ ,$$

$$\beta_\nu = -\frac{2}{\nu}C_\nu^{l,r}C_\nu^{l',r'}\ ,\quad -l'\le\nu\le r',\quad \nu\neq 0\ .$$

The constants in the theorem are given by:

$$\zeta_\nu^{l,r} = \sum_{-l\le k\le r,\ k\neq\nu}\frac{1}{\nu-k}\ ,\qquad C_\nu^{l,r} = \frac{l!r!}{(l+\nu)!(r-\nu)!}\ .$$

Spatial Order of Accuracy of HV Methods

Question:

Given a p^{th}-order HV-DDO $[\mathcal{D}_x]$, what is the (spatial) order of the corresponding HV scheme?

Case study: Advection ($w_t + w_x = 0$) of a sine wave

Spatial Order of Accuracy of HV Methods

Question:

Given a p^{th}-order HV-DDO $[\mathcal{D}_x]$, what is the (spatial) order of the corresponding HV scheme?

Case study: Advection ($w_t + w_x = 0$) of a sine wave

- Upwind finite-difference method, version 1.

$$\frac{dw_j}{dt} + \frac{1}{h}(w_j - w_{j-1}) = 0 \ ,$$

  two-point difference, first-order accurate.

- Upwind finite-difference method, version 2.

$$\frac{dw_j}{dt} + \frac{1}{2h}(3w_j - 4w_{j-1} + w_{j-2}) = 0 \ ,$$

  three-point difference, second-order accurate.

Spatial Order of Accuracy of HV Methods

Question:

Given a p^{th}-order HV-DDO $[\mathcal{D}_x]$, what is the (spatial) order of the corresponding HV scheme?

Case study: Advection ($w_t + w_x = 0$) of a sine wave

- Upwind hybrid-variable method.

$$\begin{cases} \frac{d\overline{w}_{j+1/2}}{dt} + \frac{1}{h}(w_{j+1} - w_j) = 0 \,, \\ \\ \frac{dw_j}{dt} + \frac{2}{h}(w_j - \overline{w}_{j-1/2}) = 0 \,. \end{cases}$$

  two-point difference, second-order accurate.

- This property is very general!

Spatial Order of Accuracy of HV Methods

Question:

Given a p^{th}-order HV-DDO $[\mathcal{D}_x]$, what is the (spatial) order of the corresponding HV scheme?

Case study: Advection ($w_t + w_x = 0$) of a sine wave

- Upwind hybrid-variable method.

$$\begin{cases} \frac{d\overline{w}_{j+1/2}}{dt} + \frac{1}{h}(w_{j+1} - w_j) = 0 \,, \\ \\ \frac{dw_j}{dt} + \frac{2}{h}(w_j - \overline{w}_{j-1/2}) = 0 \,. \end{cases}$$

  two-point difference, second-order accurate.

- This property is very general!

Spatial Order of Accuracy of HV Methods

Formal definition of the order of the HV methods

- Apply Fourier decomposition of $L^2([0,\ L])$ and consider simple wave $w_0(x) = e^{i\kappa x}$, $\kappa = 2\pi k/L$ for some $k \in \mathbb{Z}$; the exact data are:

$$w_j^\star(t) = e^{-ic\kappa t}e^{ij\theta}\ , \quad \overline{w}_{j+1/2}^\star(t) = \frac{1}{i\theta}e^{-ic\kappa t}e^{ij\theta}(e^{i\theta}-1)\ .$$

  $\theta = \kappa h$ is the numerical wavenumber.

- The semi-discretized HV method is an ODE system:

$$\begin{cases} \overline{w}'_{j+1/2} + \frac{1}{h}(cw_{j+1} - cw_j) = 0\ , \\ w'_j + \frac{c}{h}\left(\sum_{k=-l}^{r-1}\alpha_k\overline{w}_{j+k+1/2} + \sum_{k=-l'}^{r'}\beta_k w_{j+k}\right) = 0\ . \end{cases}$$

  Given exact initial data, the solutions to this ODE system are:

$$w_j(t) = N(t)e^{ij\theta}\ , \quad \overline{w}_{j+1/2}(t) = \frac{1}{i\theta}A(t)e^{ij\theta}(e^{i\theta}-1)\ .$$

Spatial Order of Accuracy of HV Methods

Formal definition of the order of the HV methods

- $A(t)$ and $N(t)$ are the unique solutions to the ODE system:

$$\begin{cases} A'(t) + ic\kappa N(t) = 0 \,, \\ N'(t) + c\kappa\, a(\theta)A(t) + c\kappa\, b(\theta)N(t) = 0 \,; \\ A(0) = N(0) = 1 \,, \end{cases}$$

where

$$a(\theta) = \frac{1 - e^{-i\theta}}{i\theta^2} \sum_{k=-l}^{r-1} \alpha_k e^{ik\theta} \,, \quad b(\theta) = \frac{1}{\theta} \sum_{k=-l'}^{r'} \beta_k e^{ik\theta} \,.$$

Definition

The HV method is p^{th}-order accurate if $A(t)$ and $N(t)$ satisfy:

$$A(t) = e^{-ic\kappa t}(1 + c_a(t)\theta^p + O(\theta^{p+1})) \,, \quad N(t) = e^{-ic\kappa t}(1 + c_n(t)\theta^p + O(\theta^{p+1})) \,,$$

where c_a and c_n are nonzero functions of t.

HV Methods are One-Order Higher!

Theorem

If $[\mathcal{D}_x]$ is an p^{th}-order HV-DDO and $cb_0 > 0$, where $b_0 = \beta_{-l'} + \cdots + \beta_{r'}$ is the *stability index* of the operator, then the corresponding semi-discretized HV method is $(p+1)^{\text{th}}$-order accurate.

Sketch of the proof

- Solve the ODE system for $A(t)$ and $N(t)$ by finding the eigenvalues of $\mathbf{C}(\theta)$:

$$\begin{bmatrix} A(t) \\ N(t) \end{bmatrix} = e^{-c\kappa \mathbf{C}(\theta)} \begin{bmatrix} 1 \\ 1 \end{bmatrix}, \quad \mathbf{C}(\theta) = \begin{bmatrix} 0 & i \\ a(\theta) & b(\theta) \end{bmatrix}.$$

- Asymptotic behavior of the two eigenvalues as $\theta \to 0$:

$$\lambda_1 = i - \frac{i^{p+2} c_p}{b_0} \theta^{p+1} + O(\theta^{p+2}), \quad \lambda_2 = \frac{b_0}{\theta} + O(1).$$

- Contribution of λ_2 decays exponentially as $h \to 0$ if $cb_0 > 0$:

$$e^{-c\kappa\lambda_2 t} = e^{-\frac{cb_0 t}{h}} O(1).$$

The Generalized Upwind Condition

Interpreting the condition $cb_0 > 0$

For all the HV methods where $[\mathcal{D}_x]$ is constructed on compact stencils, $cb_0 > 0$ if and only the stencil is biased towards the upwind direction.

Theorem

Let $[\mathcal{D}_x]$ be an HV-DDO with optimal accuracy on a compact stencil, then $b_0 = 0$ if and only if $l = r$ and $l' = r'$; otherwise:

- $b_0 > 0$ if and only if $l > r$ or $l = r$ and $l' > r'$.
- $b_0 < 0$ if and only if $l < r$ or $l = r$ and $l' < r'$.

- The proof utilizes the explicit coefficients given before.
- $cb_0 > 0$ is the generalized upwind condition.

Sample HV Methods

Examples of HV methods

- We assume $c > 0$ and choose operators with $b_0 > 0$.
- Fully upwind second-order HV method:

$$[\mathcal{D}_x^{\text{up-1-f}} w]_j = \frac{1}{h}\left(-2\overline{w}_{j-1/2} + 2w_j\right) .$$

- Fully upwind third-order HV method:

$$[\mathcal{D}_x^{\text{up-2-f}} w]_j = \frac{1}{h}\left(-6\overline{w}_{j-1/2} + 2w_{j-1} + 4w_j\right) .$$

- Fully upwind fourth-order HV method:

$$[\mathcal{D}_x^{\text{up-3-f}} w]_j = \frac{1}{h}\left(-\frac{1}{2}\overline{w}_{j-3/2} - \frac{17}{2}\overline{w}_{j-1/2} + 4w_{j-1} + 5w_j\right) .$$

- Upwind-biased fourth-order HV method:

$$[\mathcal{D}_x^{\text{up-3-b}} w]_j = \frac{1}{h}\left(-\frac{7}{2}\overline{w}_{j-1/2} + \frac{1}{2}\overline{w}_{j+1/2} + w_{j-1} + 2w_j\right) .$$

Sample HV Methods

Examples of HV methods

- We assume $c > 0$ and choose operators with $b_0 > 0$.
- Fully upwind fifth-order HV method (unstable):

$$[\mathcal{D}_x^{\text{up-4-f}} w]_j = \frac{1}{h}\left(-\frac{7}{2}\overline{w}_{j-3/2} - \frac{23}{2}\overline{w}_{j-1/2} + w_{j-2} + 8w_{j-1} + 6w_j\right) .$$

- Upwind-biased fifth-order HV method:

$$[\mathcal{D}_x^{\text{up-4-b}} w]_j = \frac{1}{h}\left(-\frac{1}{6}\overline{w}_{j-3/2} - \frac{31}{6}\overline{w}_{j-1/2} + \frac{1}{3}\overline{w}_{j+1/2} + 2w_{j-1} + 3w_j\right) .$$

Stability of Sample HV Methods

Linear stability analysis

- Vector form of the solution to the Cauchy problem:

$$\boldsymbol{W} = [\overline{w}_{1/2},\ \overline{w}_{3/2},\ \cdots,\ \overline{w}_{N-1/2},\ w_0,\ \cdots,\ w_{N-1}]^T\ .$$

- Matrix form of the semi-discretized system (assuming $c = 1$ and $h = 1$):

$$\frac{d\boldsymbol{W}}{dt} = \boldsymbol{D}\boldsymbol{W}\ , \quad \boldsymbol{D} = \begin{bmatrix} \boldsymbol{0} & \boldsymbol{I} - \boldsymbol{S} \\ G(\boldsymbol{S}) & H(\boldsymbol{S}) \end{bmatrix}\ ;$$

$$\boldsymbol{S} = \begin{bmatrix} 0 & 1 & \cdots & 0 & 0 \\ 0 & 0 & \cdots & 0 & 0 \\ \vdots & \vdots & \ddots & \vdots & \vdots \\ 0 & 0 & \cdots & 0 & 1 \\ 1 & 0 & \cdots & 0 & 0 \end{bmatrix}\ , \quad G(s) = -\sum_{k=-l}^{r-1} \alpha_k s^k\ , \quad H(s) = -\sum_{k=-l'}^{r'} \beta_k s^k\ .$$

Stability of Sample HV Methods

Linear stability analysis

- The ODE system is stable if:
  - $\boldsymbol{D}$ is diagonalizable.
  - All eigenvalues of $\boldsymbol{D}$ are on the closed left complex plane, and at most one on the imaginary axis.
- Define the discriminant function $\Delta(s) = H(s)^2 + 4G(s)(1-s)$.

Lemma

$\boldsymbol{D} \in \mathbb{R}^{2N \times 2N}$ is diagonalizable for all $N > 0$ if $\Delta(s) \neq 0$ for all complex number s on the unit circle.

Sketch of the proof

- $\boldsymbol{S}$ has N distinct eigenvalues on the unit circle.
- Compute all eigenvalues and eigenvectors of $\boldsymbol{D}$ using the method of tensor product.

Stability of Sample HV Methods

Linear stability analysis

- The ODE system is stable if:
  - $\boldsymbol{D}$ is diagonalizable.
  - All eigenvalues of $\boldsymbol{D}$ are on the closed left complex plane, and at most one on the imaginary axis.
- Define the discriminant function $\Delta(s) = H(s)^2 + 4G(s)(1-s)$.

Lemma

The eigenvalues of $\boldsymbol{D}$ belong to the set:

$$\mathcal{S}_{G,H} = \left\{ \frac{1}{2}(H(s) \pm \sqrt{\Delta(s)}) \ : \ s \in \mathbb{C}, \ ||s|| = 1 \right\} .$$

$\mathcal{S}_{G,H}$ belong to the left complex plane if and only if:

$$\text{(a) } \text{Re } H(s) \leq 0 \quad \text{and} \quad \text{(b) } ||\Delta(s)|| \leq ||H(s)||^2 - 4\text{Re } G(s)(1-s) ,$$

for all s on the unit circle.

Stability of Sample HV Methods

Linear stability analysis

- The ODE system is stable if:
  - $\boldsymbol{D}$ is diagonalizable.
  - All eigenvalues of $\boldsymbol{D}$ are on the closed left complex plane, and at most one on the imaginary axis.
- Define the discriminant function $\Delta(s) = H(s)^2 + 4G(s)(1-s)$.

Example: $[\mathcal{D}_x^{\textbf{up-1-f}}]$.

- $H(s) = -2$, $G(s) = 2/s$.
- $\Delta(s) = 8/s - 4 \quad \Rightarrow \quad \boldsymbol{D}$ is diagonalizable.
- (a) holds naturally.
- (b) is equivalent to:

$$0 \leq 64(1-\rho)^2 \ ,$$

where $\rho = \mathrm{Re}\ s$.

Stability of Sample HV Methods

Linear stability analysis

- The ODE system is stable if:
  - $\boldsymbol{D}$ is diagonalizable.
  - All eigenvalues of $\boldsymbol{D}$ are on the closed left complex plane, and at most one on the imaginary axis.
- Define the discriminant function $\Delta(s) = H(s)^2 + 4G(s)(1-s)$.

Example: $[\mathcal{D}_x^{\mathbf{up\text{-}4\text{-}b}}]$.

- $H(s) = -3 - 2s^{-1}$, $G(s) = -\frac{1}{3} + \frac{31}{6}s^{-1} + \frac{1}{6}s^{-2}$.
- $\Delta(s) = \frac{14}{3}s^{-2} + 32s^{-1} - 13 + \frac{4}{3}s$. For all $||s|| = 1$, $||\Delta(s)||^2 = \frac{1}{9}(448\rho^3 - 648\rho^2 - 5448\rho + 11273) > 0$; hence $\boldsymbol{D}$ is diagonalizable.
- $\mathrm{Re}\, H(s) = -3 - 2\rho$: (a) holds.
- (b) is equivalent to:

$$0 \leq 16(1-\rho)^3(11-\rho)\ ,$$

and we have stability.

Stability of Sample HV Methods

Linear stability analysis

- The ODE system is stable if:
  - $\boldsymbol{D}$ is diagonalizable.
  - All eigenvalues of $\boldsymbol{D}$ are on the closed left complex plane, and at most one on the imaginary axis.
- Define the discriminant function $\Delta(s) = H(s)^2 + 4G(s)(1-s)$.

Example: $[\mathcal{D}_x^{\textbf{up-4-f}}]$.

- $H(s) = -6 - 8s^{-1} - s^{-2}$, $G(s) = \frac{23}{2}s^{-1} + \frac{7}{2}s^{-2}$.
- $\Delta(s) = s^{-4} + 16s^{-3} + 90s^{-2} + 128s^{-1} - 10$ has no roots on the unit circle. $\boldsymbol{D}$ is diagonalizable.
- As $s \to -1$, $\operatorname{Re} H(s) \to 1 > 0$; hence this method is unstable.

Stability of Sample HV Methods

Linear stability analysis

- The ODE system is stable if:
  - $\boldsymbol{D}$ is diagonalizable.
  - All eigenvalues of $\boldsymbol{D}$ are on the closed left complex plane, and at most one on the imaginary axis.
- Define the discriminant function $\Delta(s) = H(s)^2 + 4G(s)(1-s)$.

Stable fully-discretized HV methods and Courant numbers $\nu_{\max}$

- Explicit Runge-Kutta methods.
- Courant number: $\Delta t \leq \nu_{\max} h / |c|$.
- 2^{nd}-order: $[\mathcal{D}_x^{\text{up-1-f}}]$ and RK2, $\nu_{\max} = 1.0$.
- 3^{nd}-order: $[\mathcal{D}_x^{\text{up-2-f}}]$ and RK3, $\nu_{\max} = 0.409$.
- 4^{nd}-order: $[\mathcal{D}_x^{\text{up-3-f}}]$ and RK4, $\nu_{\max} = 0.309$.
- 4^{nd}-order: $[\mathcal{D}_x^{\text{up-3-b}}]$ and RK4, $\nu_{\max} = 0.808$.
- 5^{nd}-order: $[\mathcal{D}_x^{\text{up-4-b}}]$ and RK5, $\nu_{\max} = 0.494$.

Introduction to Order Stars

When are HV methods stable?

- Not all upwind methods are linearly stable, such as $[\mathcal{D}_x^{\text{up-4-f}}]$.
- For finite-difference methods, the upwind stencil cannot contain more than two points than the downwind stencil.

Theorem (Iserles and Strang, 1983)

Consider the finite difference method given by the discrete differential operator $\mathcal{D}_x$:

$$\frac{dw_j}{dt} + c\mathcal{D}_x w_j = 0 \,, \quad \mathcal{D}_x w_j = \frac{1}{h} \sum_{k=-l'}^{r'} \beta_k w_{j+k} \,,$$

where $\mathcal{D}_x$ is of optimal order of accuracy $l' + r'$. Assuming $c > 0$, the corresponding finite-difference method is linearly stable if and only if $r' \leq l' \leq r' + 2$.

Introduction to Order Stars

Order stars

- The order star is a very romantic name for a special class of holomorphic functions that connects the order of accuracy and linear stability.
- Characteristic function of an FD operator:

$$\mu - H(e^z) = 0\,, \quad H(s) = -\sum_{k=-l'}^{r'} \beta_k s^k\,.$$

- The FD method is p^{th}-order accurate:

$$\sigma(z) = \mu - z = H(e^z) - z \sim C_{p+1} z^{p+1}$$

as $z \to 0$, where $C_{p+1} \neq 0$ is some constant.

- The FD method is linearly stable if:

$$(-i\pi,\ i\pi] \subset \mathcal{D} = \{z \in \mathcal{S}\ :\ \mathrm{Re}\ \sigma(z) \geq 0\ \}.$$

where $\mathcal{D}$ is called the *stability domain* of the method and $\mathcal{S}$ is the tube that equates $x + iy$ with $x + i(y + 2\pi)$.

Introduction to Order Stars

Examples of order stars

1^{st}-order: $\mathcal{D}_x w_j = (w_j - w_{j-1})/h$ – stable

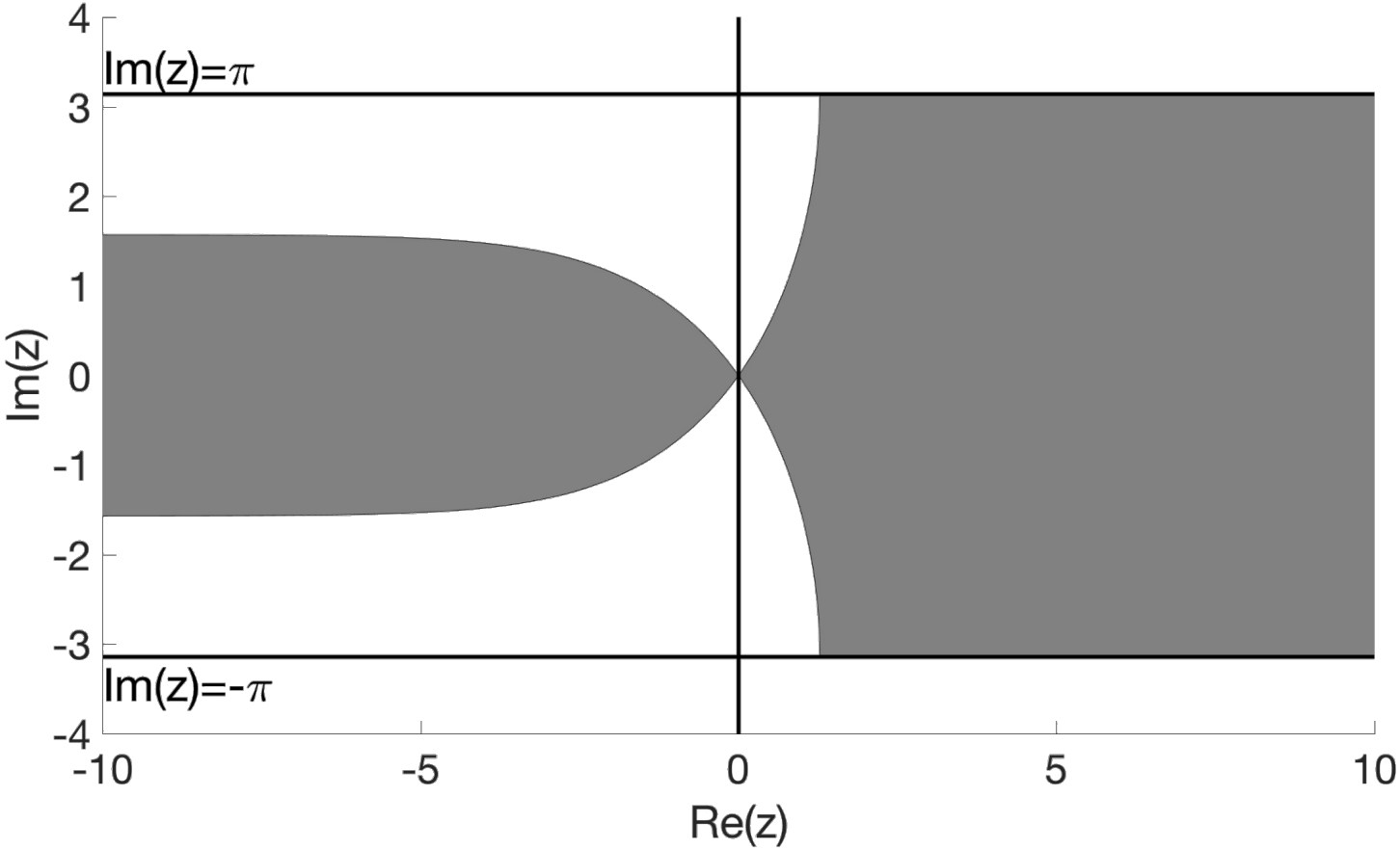

Introduction to Order Stars

Examples of order stars

2^{nd}-order: $\mathcal{D}_x w_j = (3w_j - 4w_{j-1} + w_{j-2})/(2h)$ – stable

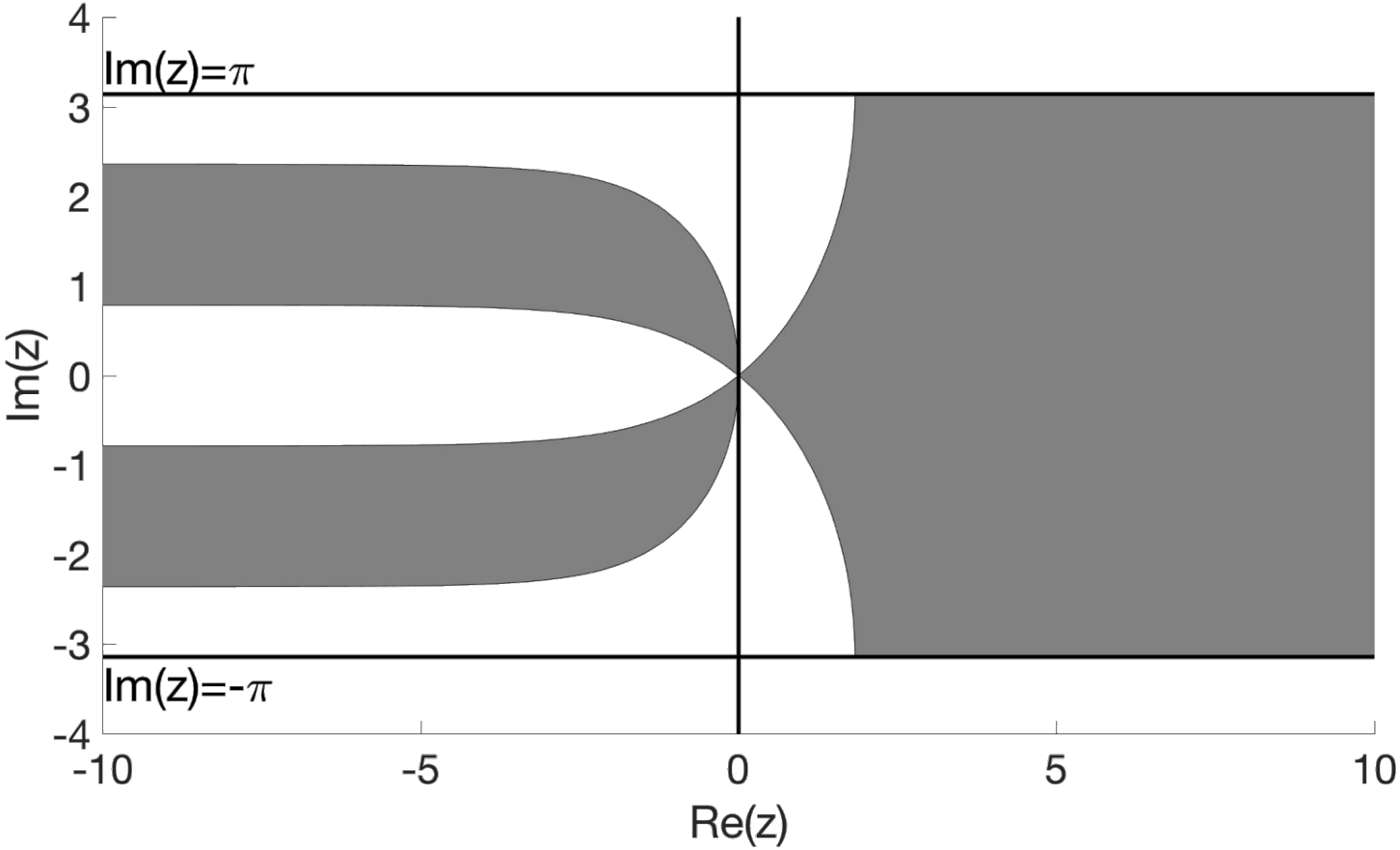

Introduction to Order Stars

Examples of order stars

3^{rd}-order: $\mathcal{D}_x w_j = (11w_j - 18w_{j-1} + 9w_{j-2} - 2w_{j-3})/(6h)$ – unstable

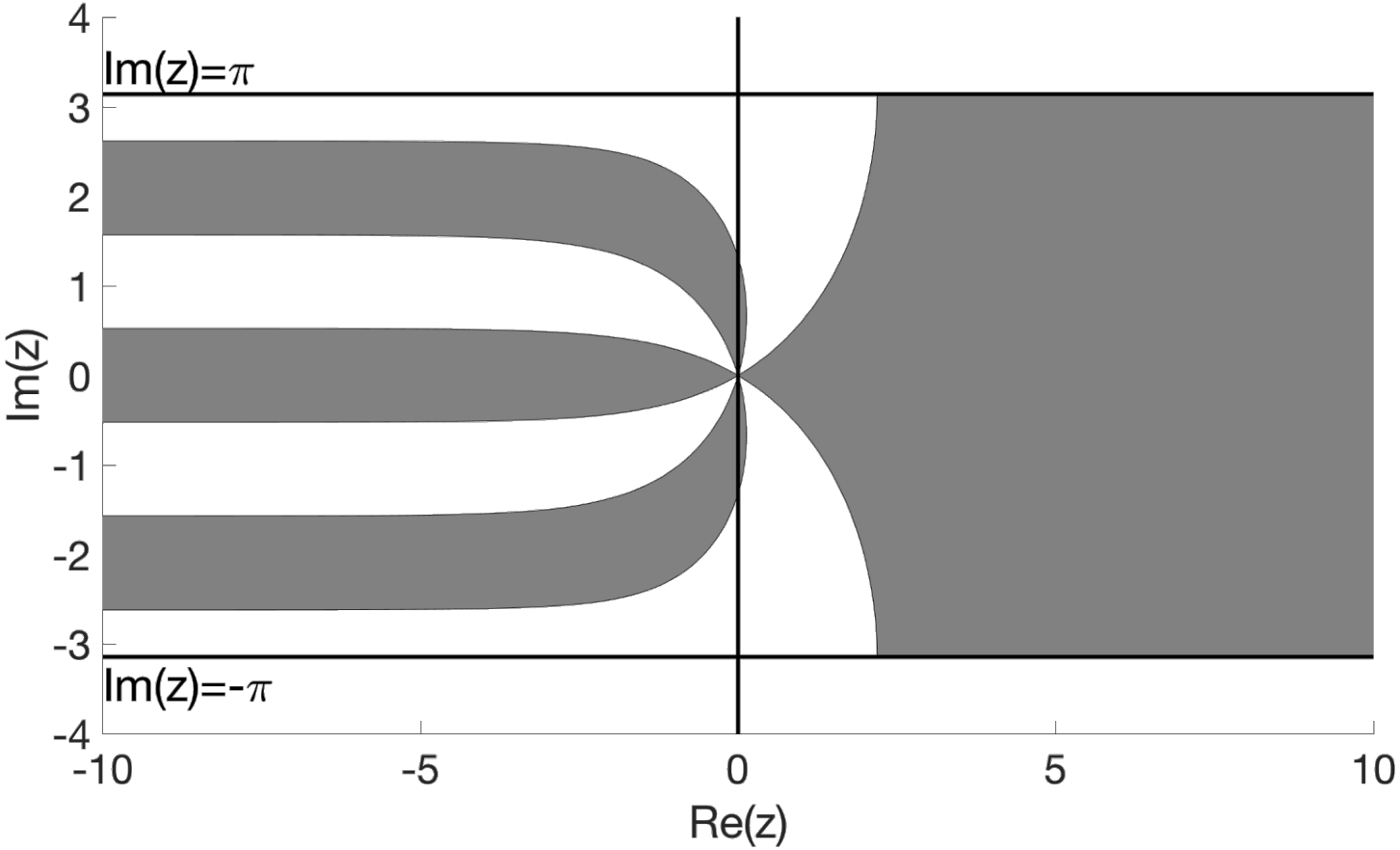

Introduction to Order Stars

Examples of order stars

3^{rd}-order: $\mathcal{D}_x w_j = (2w_{j+1} + 3w_j - 6w_{j-1} + w_{j-2})/(6h)$ – stable

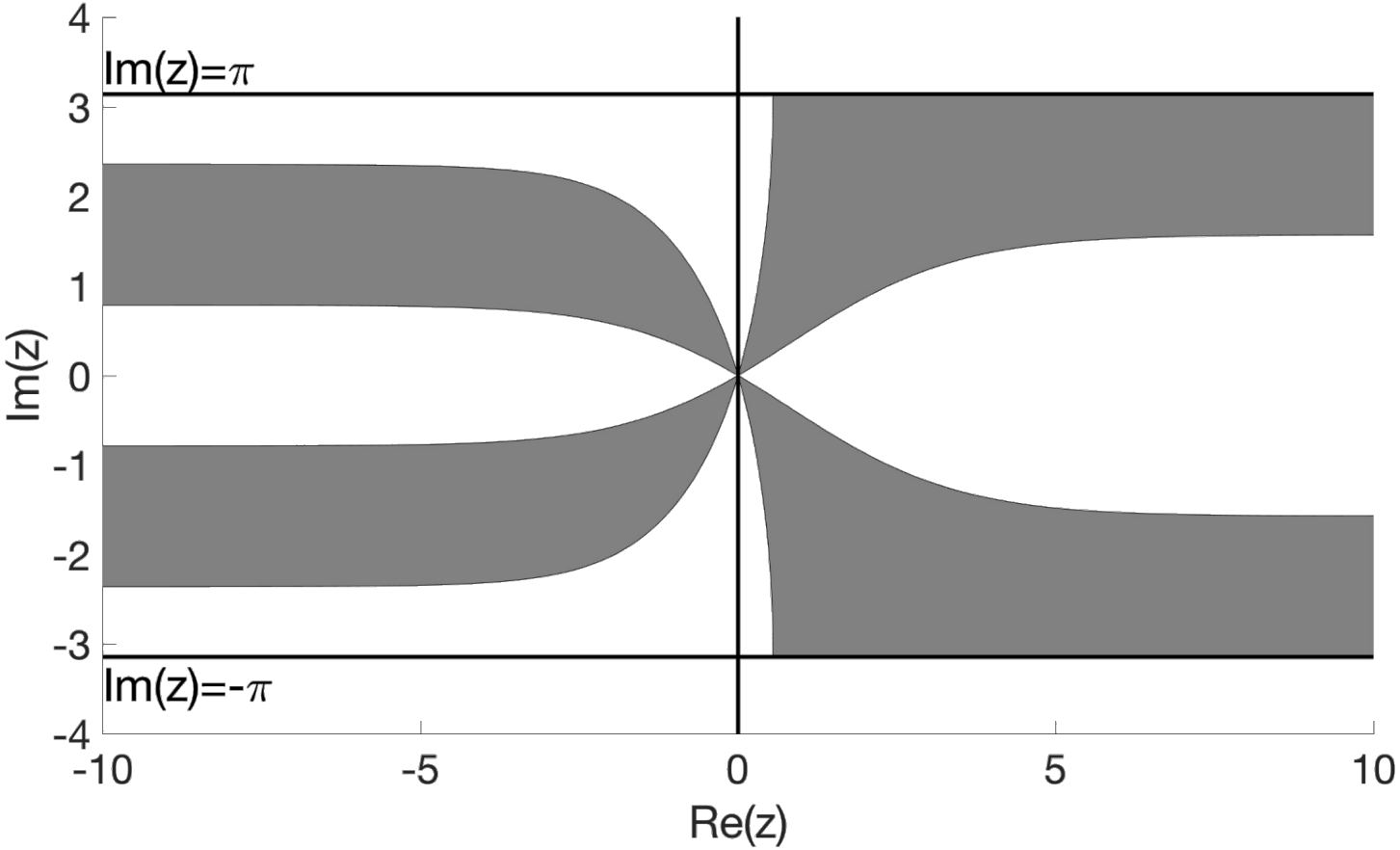

Introduction to Order Stars

Stencil barrier

- Near $z = 0$, the order star $\mathcal{O} = \mathcal{S} \backslash \overline{\mathcal{D}}$ is composed of $p + 1$ sections with equal angle $\pi/(p + 1)$.
- The curves of $\partial\mathcal{O}$ as $\mathrm{Re}\, z \to +\infty$ is determined by the right stencil r'.

$$\mathrm{Re}\, \sigma(z) \sim \beta_{r'} e^{r'x + ir'y} - (x + iy) \ .$$

- The curves of $\partial\mathcal{O}$ as $\mathrm{Re}\, z \to -\infty$ is determined by the left stencil l'.

$$\mathrm{Re}\, \sigma(z) \sim \beta_{-l'} e^{-l'x - il'y} - (x + iy) \ .$$

- One thusly obtains the stencil (order) barrier by Iserles and Strang.

Riemann Surfaces that Characterize the HV Methods

Order stars for HV methods

- Characteristic function of an HV-DDO:

$$\mu^2 - H(e^z)\mu - (1 - e^z)G(e^z) = 0 \ .$$

- It describes a holomorphic function on a Riemann surface:

$$\mathcal{M} = \{\boldsymbol{z} = (z, \mu) \in \mathcal{S} \times \mathbb{C} \ : \ \mu^2 - H(e^z)\mu - (1 - e^z)G(e^z) = 0 \} \ ,$$

  associated with projections: $\rho(\boldsymbol{z}) = z$ and $E(\boldsymbol{z}) = \mu$.

- Stability domain $\mathcal{D}$ and the order star $\mathcal{O} = \mathcal{M} \backslash \overline{\mathcal{D}}$.

$$\mathcal{D} = \{\boldsymbol{z} \in \mathcal{M} : \ \mathrm{Re}\, \sigma(\boldsymbol{z}) \geq 0, \ \text{if } \rho(\boldsymbol{z}) \in \mathcal{S} \backslash \mathcal{B}; \ \mathrm{Re}\, \sigma(\boldsymbol{z}) > 0, \ \text{if } \rho(\boldsymbol{z}) \in \mathcal{B}\} \ ,$$

  where $\sigma(\boldsymbol{z}) = E(\boldsymbol{z}) - \rho(\boldsymbol{z})$ and $\mathcal{B}$ is the set of branch points.

Riemann Surfaces that Characterize the HV Methods

Order stars for HV methods

$$[\mathcal{D}_x^{\text{up-1-f}}]:\ \mu^2 - (4 + 2e^{-z})\mu + 6(1 - e^{-z}) = 0$$

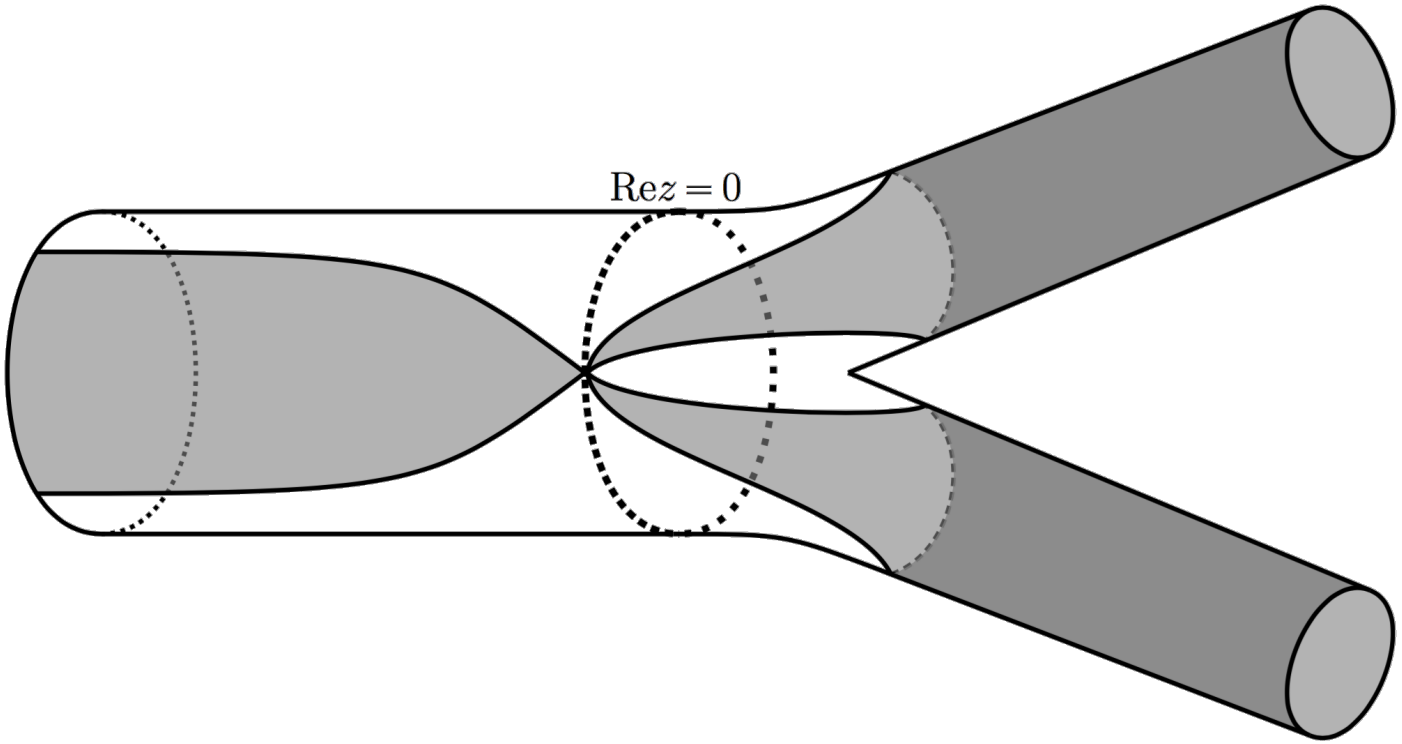

Riemann Surfaces that Characterize the HV Methods

Order stars for HV methods

$$[\mathcal{D}_x^{\text{up-1-f}}]:\ \mu^2 - (4 + 2e^{-z})\mu + 6(1 - e^{-z}) = 0$$

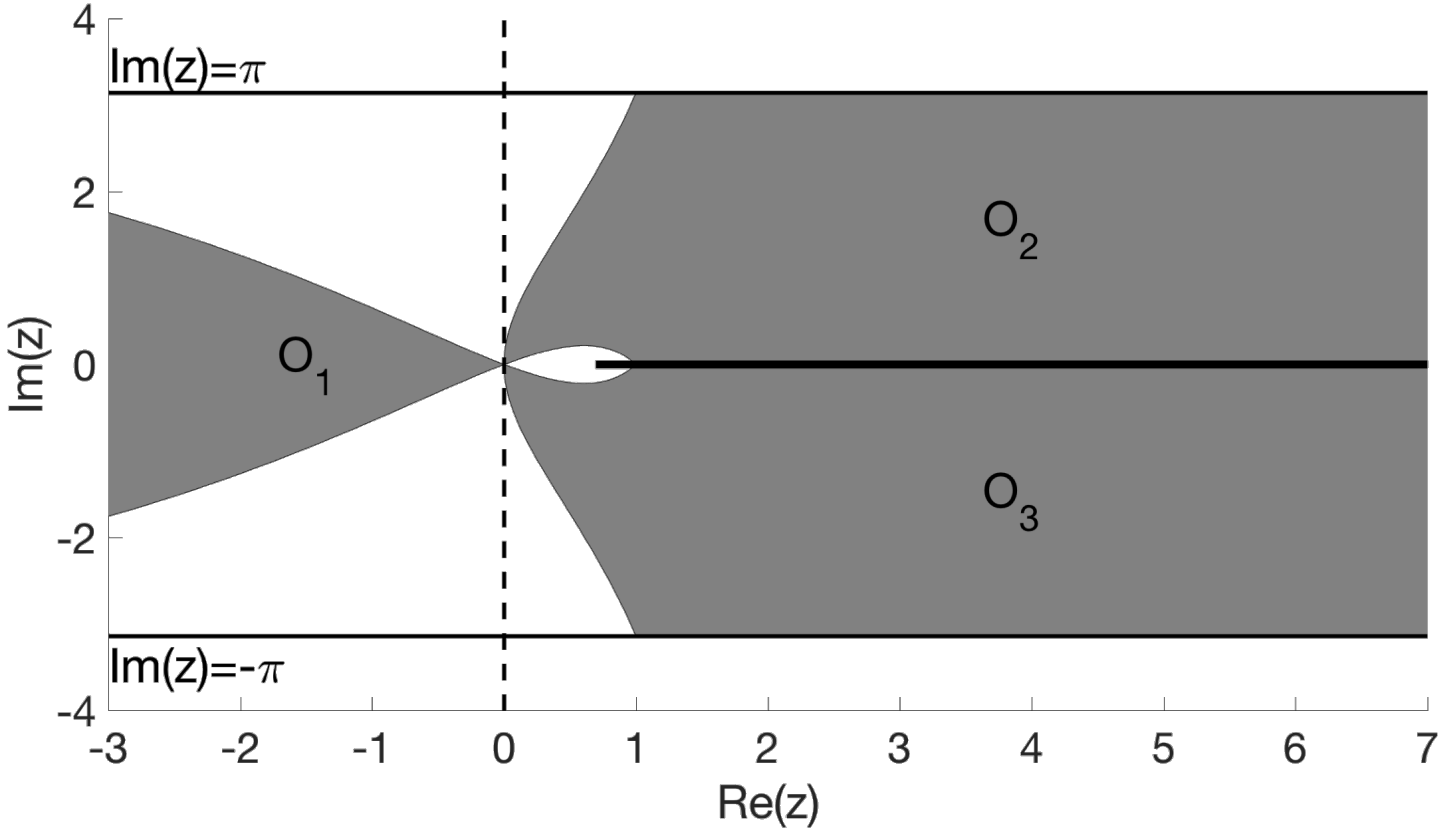

Riemann Surfaces that Characterize the HV Methods

Order stars for HV methods

$$[\mathcal{D}_x^{\text{up-1-f}}]:\ \mu^2 - (4 + 2e^{-z})\mu + 6(1 - e^{-z}) = 0$$

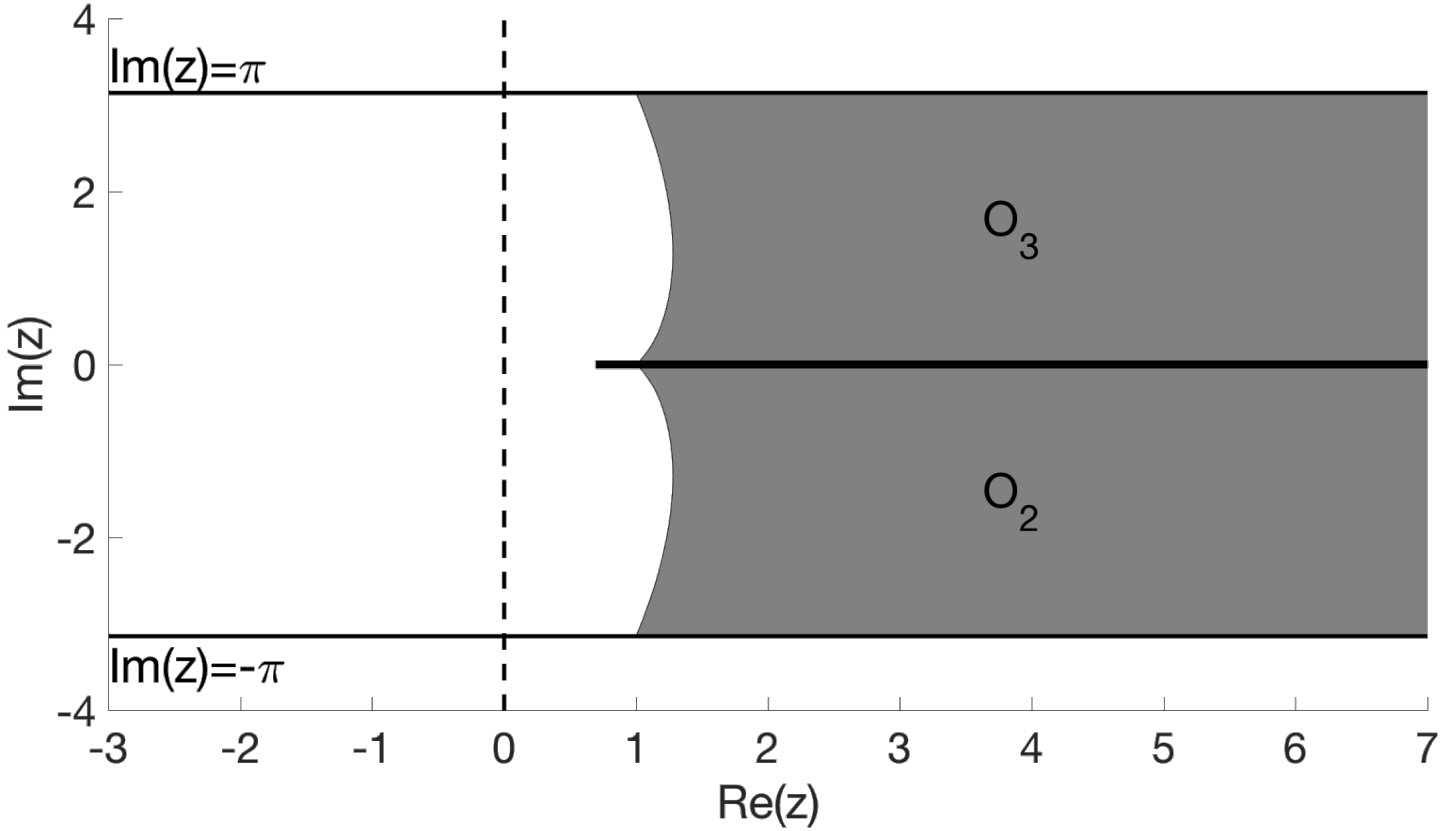

Riemann Surfaces that Characterize the HV Methods

Order stars for HV methods

$$[\mathcal{D}_x^{\text{up-3-b}}]:\ 2\mu^2 - (4 + 2e^{-z})\mu - (e^z - 8 + 7e^{-z}) = 0$$

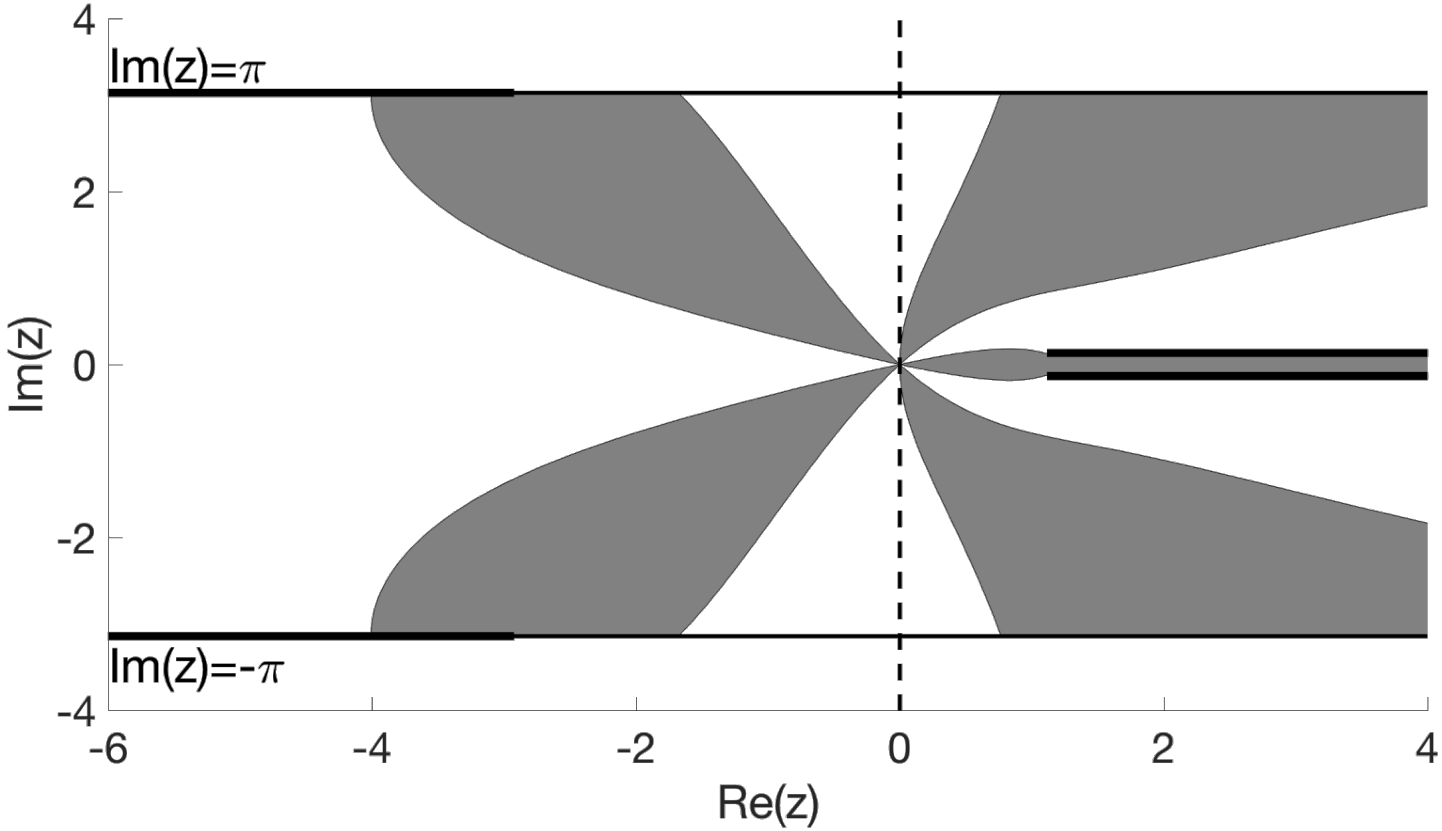

Riemann Surfaces that Characterize the HV Methods

Order stars for HV methods

$$[\mathcal{D}_x^{\text{up-3-b}}]:\ 2\mu^2 - (4 + 2e^{-z})\mu - (e^z - 8 + 7e^{-z}) = 0$$

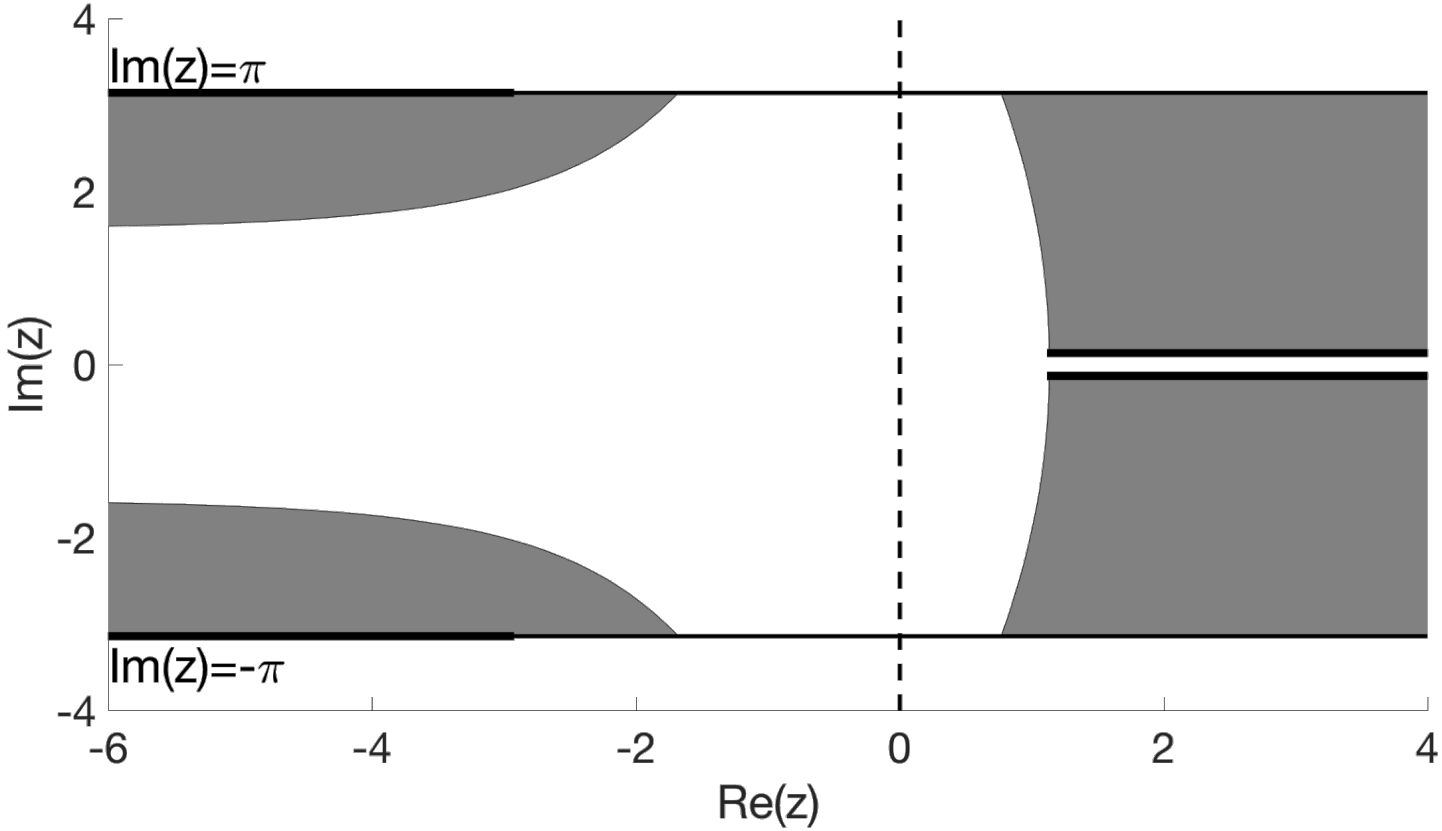

Riemann Surfaces that Characterize the HV Methods

Order stars for HV methods

$$[\mathcal{D}_x^{\text{up-4-f}}]:\ 2\mu^2 - (12 + 16e^{-z} + 2e^{-2z})\mu - (-23 + 16e^{-z} + 7e^{-2z}) = 0$$

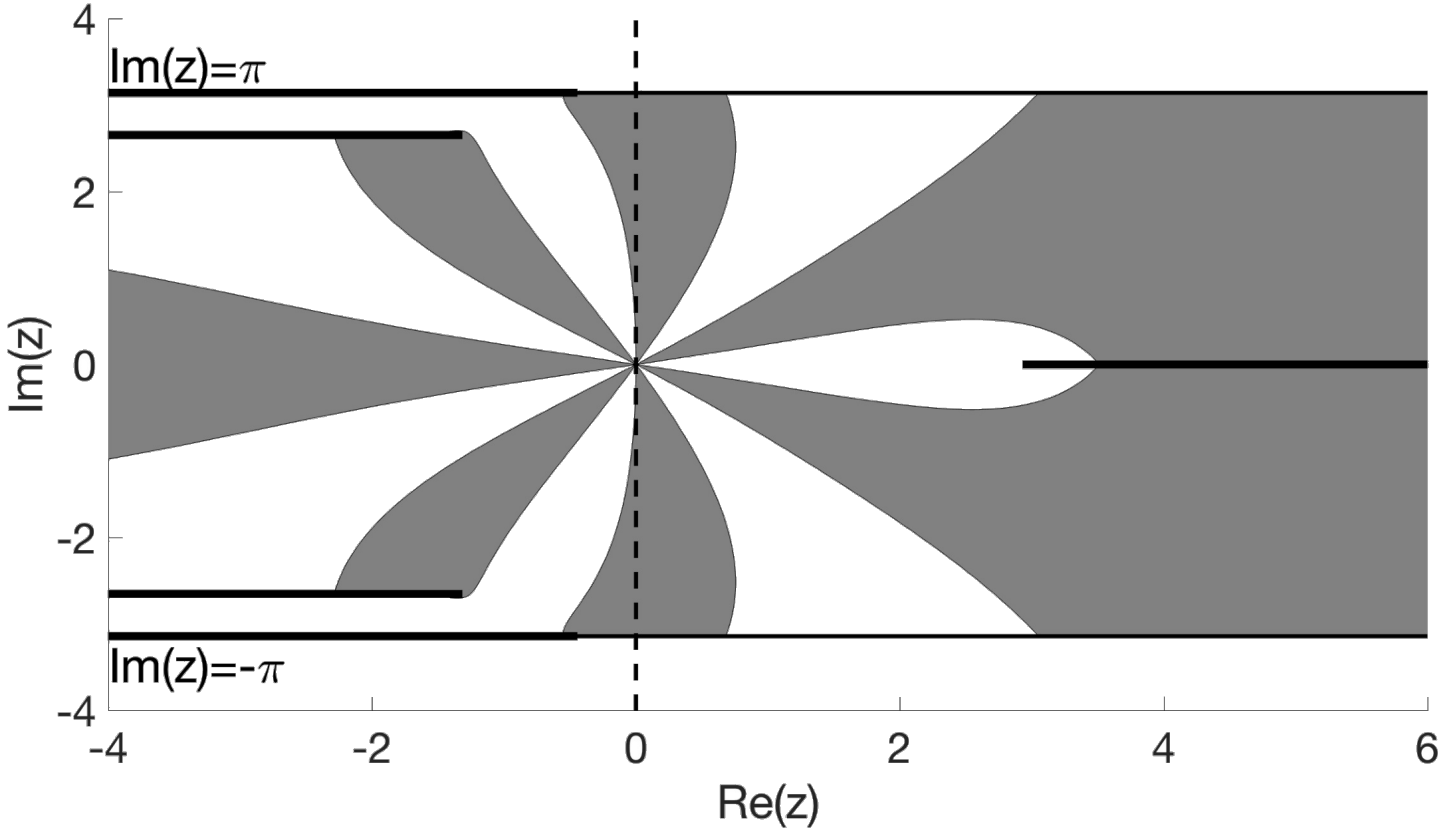

Riemann Surfaces that Characterize the HV Methods

Order stars for HV methods

$$[\mathcal{D}_x^{\text{up-4-f}}]:\ 2\mu^2 - (12 + 16e^{-z} + 2e^{-2z})\mu - (-23 + 16e^{-z} + 7e^{-2z}) = 0$$

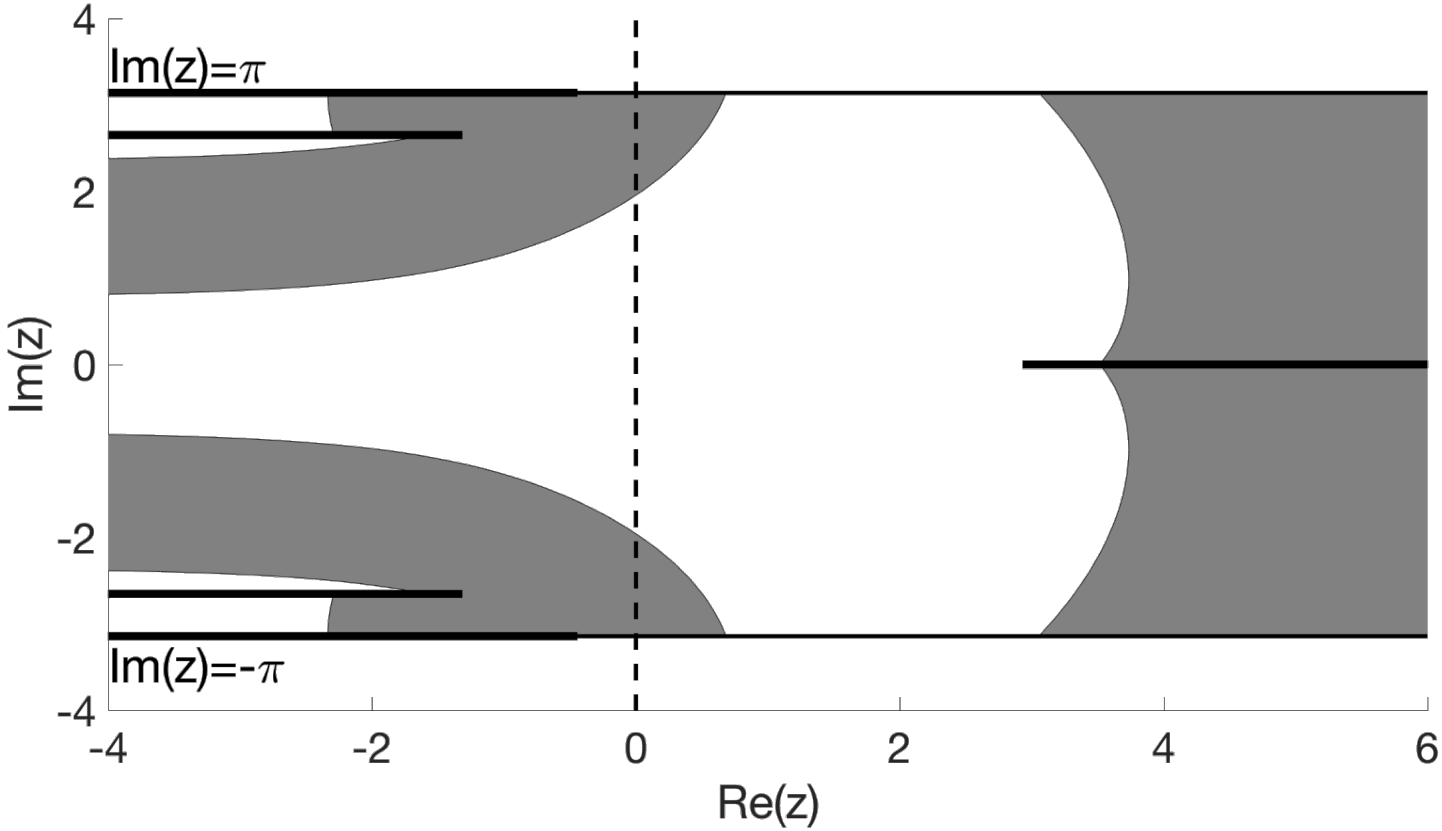

Stencil Barrier for Linearly Stable HV Methods

Stencil barrier for HV methods

- Suppose the HV-DDO is p^{th}-order accurate, and the HV method is $(p+1)^{\text{th}}$-order accurate and linearly stable.
- The number of sections of $\mathcal{O}$ near $\boldsymbol{z} = (0,0)$ is between $(p+1)/2$ and $(p+3)/2$ in both the left part of $\mathcal{M}$ and the right part.
- There are $2R$ curves of $\partial\mathcal{O}$ in the right part, $(p+1)/2 \le R \le (p+3)/2$:
  - Loops: $2C_R$, $C_R \ge 0$.
  - Infinite curves: $2r$.
- There are $2L$ curves of $\partial\mathcal{O}$ in the right part, $(p+1)/2 \le L \le (p+3)/2$:
  - Loops: $2C_L$, $C_L \ge 0$.
  - Infinite curves: $2l$.
- Using argument principle, the two numbers C_R and C_L has tight relation to the number of roots of:

$$\Delta(s) = H(s)^2 + 4G(s)(1-s) = 0\ .$$

Stencil Barrier for Linearly Stable HV Methods

Stencil barrier for HV methods

- Define:

$$
\begin{aligned}
N^{+}_{\mathbb{R},+} &: \text{ Real positive roots with modulus larger than one} \\
N^{+}_{\mathbb{R},-} &: \text{ Real negative roots with modulus larger than one} \\
N^{+}_{\mathbb{C}} &: \text{ Non-real complex roots with modulus larger than one} \\
N^{-}_{\mathbb{R},+} &: \text{ Real positive roots with modulus smaller than one} \\
N^{-}_{\mathbb{R},-} &: \text{ Real negative roots with modulus smaller than one} \\
N^{-}_{\mathbb{C}} &: \text{ Non-real complex roots with modulus smaller than one}
\end{aligned}
$$

Stencil Barrier for Linearly Stable HV Methods

Stencil barrier for HV methods

- Counting the loops:

$$N^+_{\mathbb{R},+} + N^+_{\mathbb{R},-} + N^+_{\mathbb{C}} + N^-_{\mathbb{R},+} + N^-_{\mathbb{R},-} + N^-_{\mathbb{C}} = \max(2r', r) + \max(2l', l)$$

$$C_R = 2\left\lfloor \frac{N^+_{\mathbb{R},+}+1}{2} \right\rfloor + \left\lfloor \frac{N^+_{\mathbb{R},-}+1}{2} \right\rfloor + N^+_{\mathbb{C}}$$

$$C_L = 2\left\lfloor \frac{N^-_{\mathbb{R},+}+1}{2} \right\rfloor + \left\lfloor \frac{N^-_{\mathbb{R},-}+1}{2} \right\rfloor + \frac{N^-_{\mathbb{C}}}{2} \ .$$

Stencil Barrier for Linearly Stable HV Methods

Stencil barrier for HV methods

- Counting the loops:

$$N^+_{\mathbb{R},+} + N^+_{\mathbb{R},-} + N^+_{\mathbb{C}} + N^-_{\mathbb{R},+} + N^-_{\mathbb{R},-} + N^-_{\mathbb{C}} = \max(2r', r) + \max(2l', l)$$

$$C_R = 2\left\lfloor \frac{N^+_{\mathbb{R},+}+1}{2} \right\rfloor + \left\lfloor \frac{N^+_{\mathbb{R},-}+1}{2} \right\rfloor + N^+_{\mathbb{C}}$$

$$C_L = 2\left\lfloor \frac{N^-_{\mathbb{R},+}+1}{2} \right\rfloor + \left\lfloor \frac{N^-_{\mathbb{R},-}+1}{2} \right\rfloor + \frac{N^-_{\mathbb{C}}}{2} \ .$$

Lemma

If the HV method is linearly stable and $\Delta(s)$ has no roots on the unit circle, then:

$$N^-_{\mathbb{R},+} + N^+_{\mathbb{R},+} + N^+_{\mathbb{C}} \leq 4 + 2(r - r') + 2(l - l') \ .$$

The plan for the next step is to use this lemma to establish a tighter constraint on the stencil of linearly stable HV methods.

Initial Boundary Value Problems

Modified HV-DDO near boundaries

- Initial boundary value problem for right-going advection ($c > 0$):

$$\begin{cases} w_t + cw_x = 0 \,, & (x,t) \in [0,\ L] \times \mathbb{R}^+ \\ w(x,0) = w_{\text{init}}(x) \,, & x \in [0,\ L] \\ w(0,t) = f(t) \,, & t \in \mathbb{R}^+ \,. \end{cases}$$

- Applying the chosen $[\mathcal{D}_x]$ at nodes near the two boundaries may require variables out of the domain.
- For example consider $[\mathcal{D}_x^{\text{up-4-b}}]$:

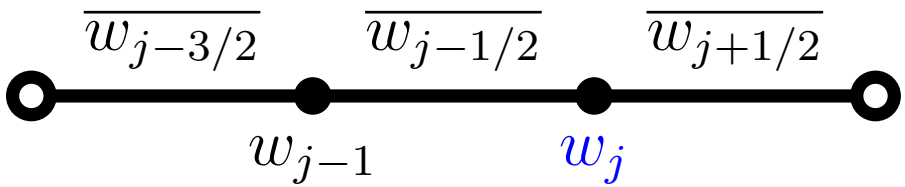

- Set $w_0(t) = f(t)$, and modify the operators at w_1 and w_N:

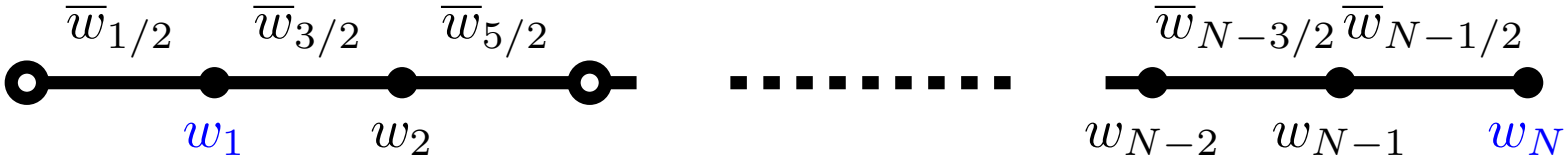

Nonlinear Conservation Systems

Characteristic decomposition for hyperbolic systems

- One-dimensional hyperbolic conservation law, where $\boldsymbol{f} : \mathbb{R}^d \to \mathbb{R}^d$:
$$\boldsymbol{w}_t + \boldsymbol{f}(\boldsymbol{w})_x = 0 \, .$$
Cell averages: $\overline{\boldsymbol{w}}_{j+1/2}$; nodal values: $\boldsymbol{w}_j$.
- Semi-discretization for cell averages:
$$\frac{d\overline{\boldsymbol{w}}_{j+1/2}}{dt} + \frac{1}{h}(\boldsymbol{f}(\boldsymbol{w}_{j+1}) - \boldsymbol{f}(\boldsymbol{w}_j)) = 0 \, .$$
- Eigenvalue decomposition of the Jacobian matrix:
$$\boldsymbol{J}(\boldsymbol{w}) = \frac{\partial \boldsymbol{f}}{\partial \boldsymbol{w}} = \boldsymbol{L}(\boldsymbol{w})^{-1} \boldsymbol{\Lambda}(\boldsymbol{w}) \boldsymbol{L}(\boldsymbol{w}) \, .$$
- Linearize around $\boldsymbol{w}_j$ for semi-discretization:
$$(\boldsymbol{L}_j \boldsymbol{w})_t + \boldsymbol{\Lambda}_j (\boldsymbol{L}_j \boldsymbol{w})_x = 0 \, .$$
- Let $\boldsymbol{L} = [\boldsymbol{l}_1 \; \boldsymbol{l}_2 \; \cdots, \; \boldsymbol{l}_d]^T$, apply the chose $[\mathcal{D}_x]$ to each characteristic:
$$(\boldsymbol{l}_{k,j}^T \boldsymbol{w})_t + \lambda_{k,j} (\boldsymbol{l}_{k,j}^T \boldsymbol{w})_x = 0 \, , \quad 1 \le k \le d \, .$$

Two Space Dimensions

Two-dimensional Cartesian grids

- The cell average $\overline{w}_{j+1/2,k+1/2}$ represents the mean solution over $[x_j,\ x_{j+1}] \times [y_k,\ y_{k+1}]$.
- The nodal variables are selected on the edges for sufficiently accurate evaluations of edge integrals.
- Sample HV methods:

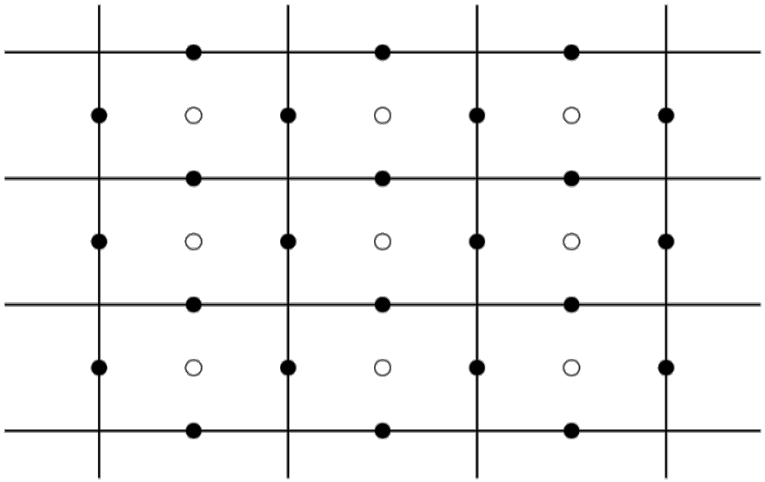

A 2^{nd}-order HV method.

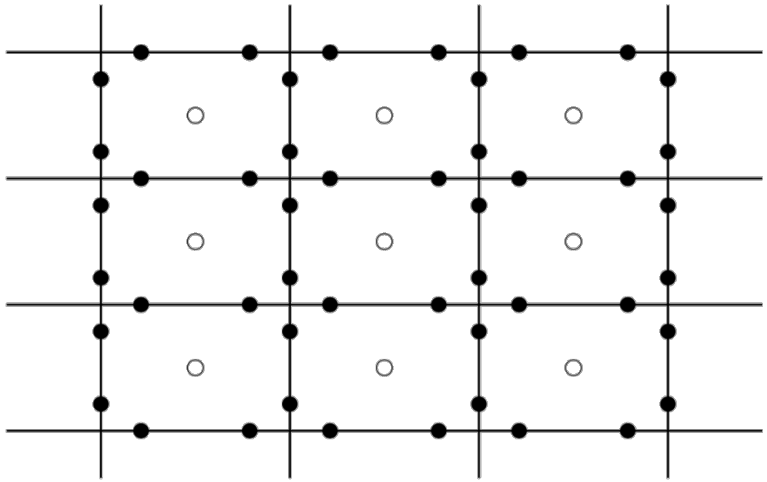

A 3^{rd}-order HV method.

One-Dimensional Problems

Linear advection equation (Cauchy problem)

- Cauchy problem:

$$\begin{cases} w_t + 2w_x = 0 \,, & (x,t) \in [-1,\ 1] \times [0,\ 1] \\ w(x,0) = 1 + \frac{1}{2}\sin(\pi\ x) \,, & x \in [-1,\ 1] \\ w(-1,t) = w(1,t) \,, & t \in [0,\ 1] \,. \end{cases}$$

- All five linearly stable HV methods.
- Four uniform grids with number of cells: 20, 40, 80, and 160.
- Courant number selected as $0.9\nu_{\max}$.

One-Dimensional Problems

Linear advection equation (Cauchy problem)

L_1-errors in cell averages (left) and nodal values (right) in logarithmic scales.

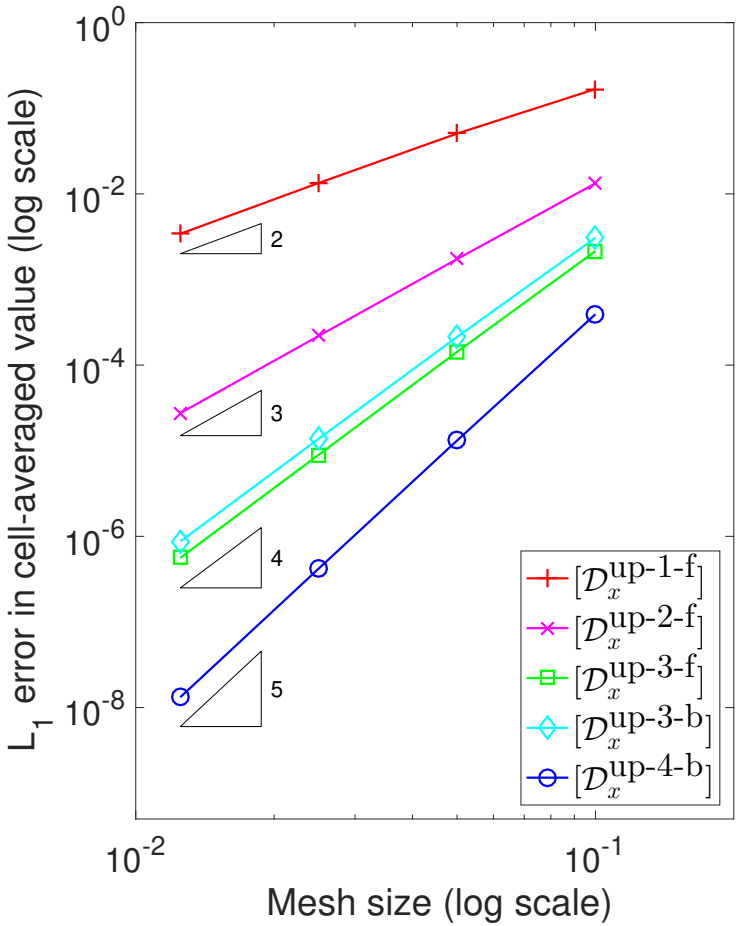

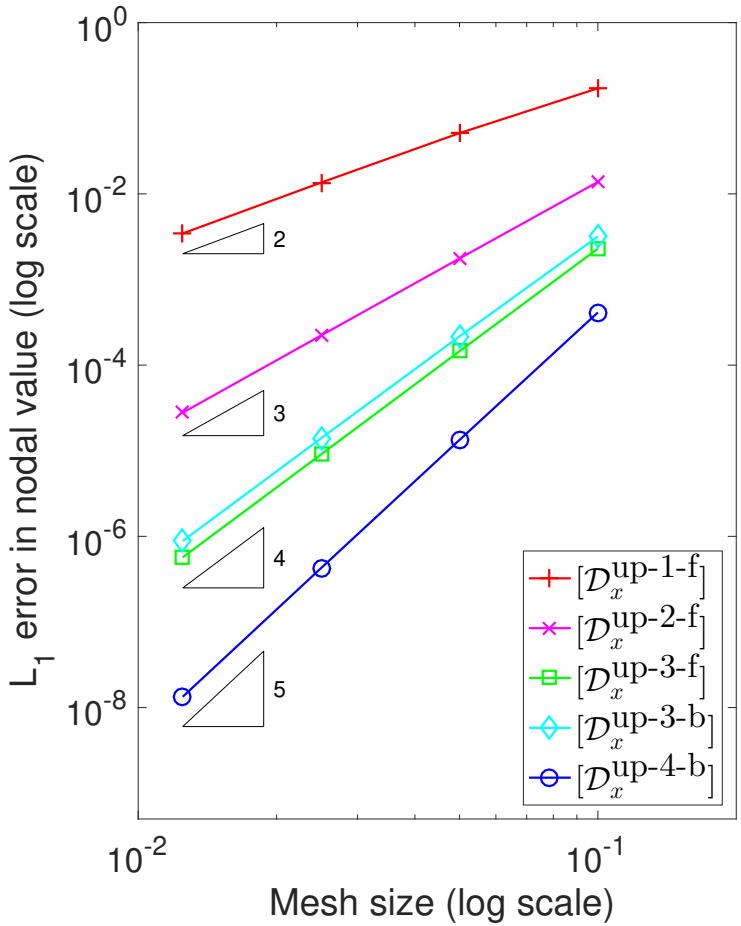

One-Dimensional Problems

Linear advection equation (IBVP)

- Initial boundary value problem:

$$\begin{cases} w_t + w_x = 0 \,, & x \in [-0.5,\ 0.5] \\ & t \in [0,\ 0.5] \\ w(x,0) = 1 + \frac{1}{2}x^3 \sin(\pi\ x) \,, & x \in [-0.5,\ 0] \\ w(x,0) = 1 \,, & x \in [0,\ 0.5] \\ w(-0.5,t) = 1 + \frac{1}{2}(t+\frac{1}{2})^3 \sin(2\pi(t+\frac{1}{2})) \,, & t \in [0,\ 0.5] \,. \end{cases}$$

- All five linearly stable HV methods with appropriate boundary modifications if necessary.
- Four uniform grids with number of cells: 20, 40, 80, and 160.
- Courant number selected as $0.9\nu_{\max}$.

One-Dimensional Problems

Linear advection equation (IBVP)

L_1-errors in cell averages (left) and nodal values (right) in logarithmic scales.

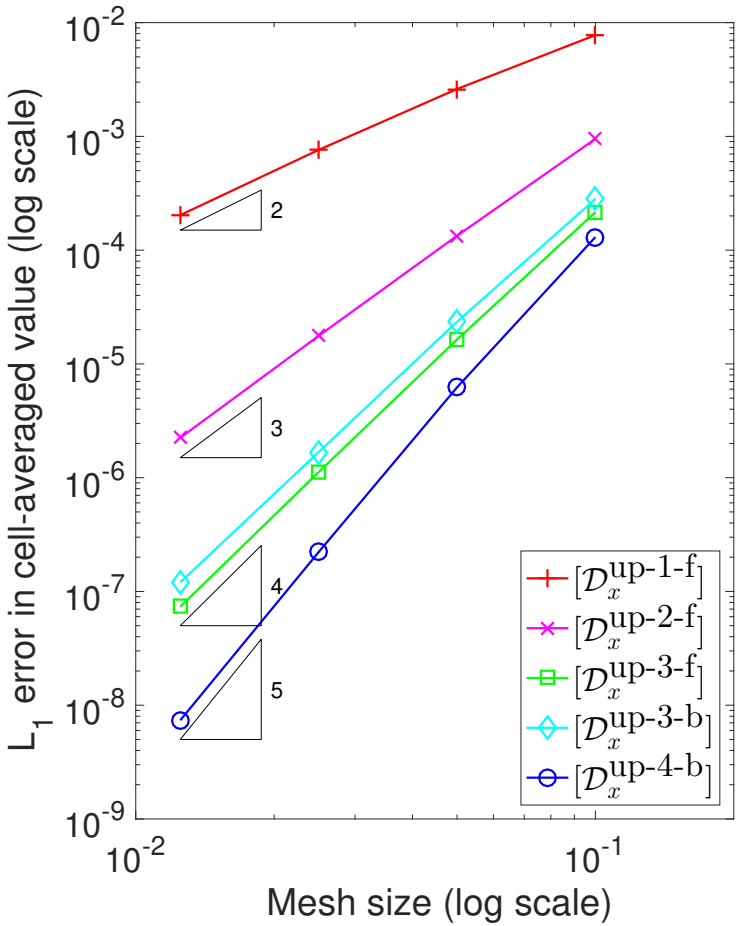

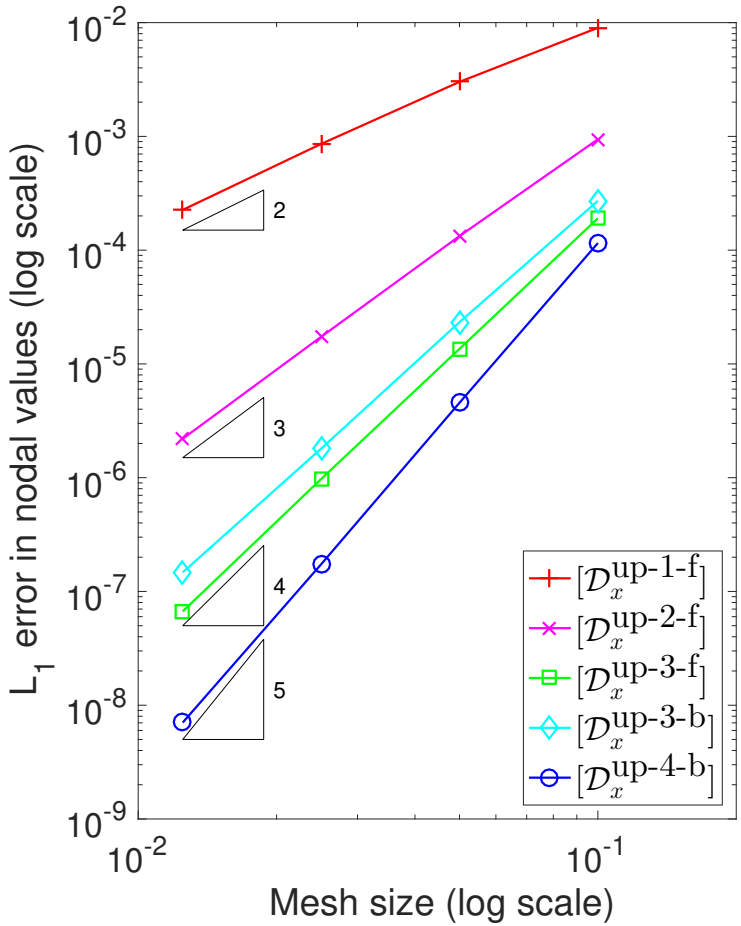

One-Dimensional Problems

Euler equations with periodic boundaries

- 1D Euler equations:

$$\begin{bmatrix} \rho \\ \rho u \\ E \end{bmatrix}_t + \begin{bmatrix} \rho u \\ \rho u^2 + p \\ (E+p)u \end{bmatrix}_x = 0\,; \quad E = \frac{p}{\gamma - 1} + \frac{1}{2}\rho u^2\,, \quad \gamma = 1.4\,.$$

- Initial condition on the interval $[-1,\ 1]$:

$$\begin{cases} \rho(x,0) = 1 + \frac{1}{2}\sin(\pi x) \\ u(x,0) = 2 + \frac{1}{2}\sin(\pi x) \\ p(x,0) = 1 + \frac{1}{2}\sin(\pi x)\,. \end{cases}$$

- Periodic boundary condition.
- Reference solutions at $T = 0.3$ are computed by $[\mathcal{D}_x^{\text{up-4-b}}]$ on a uniform mesh with $2{,}560$ cells.
- All five HV methods are tested on a sequence of grids with 40, 80, 160, and 320 cells; the Courant number is chosen as $0.9\nu_{\max}$.

One-Dimensional Problems

Euler equations with periodic boundaries

L_1-errors in $\overline{\rho}$ (left) and ρ (right) in logarithmic scales.

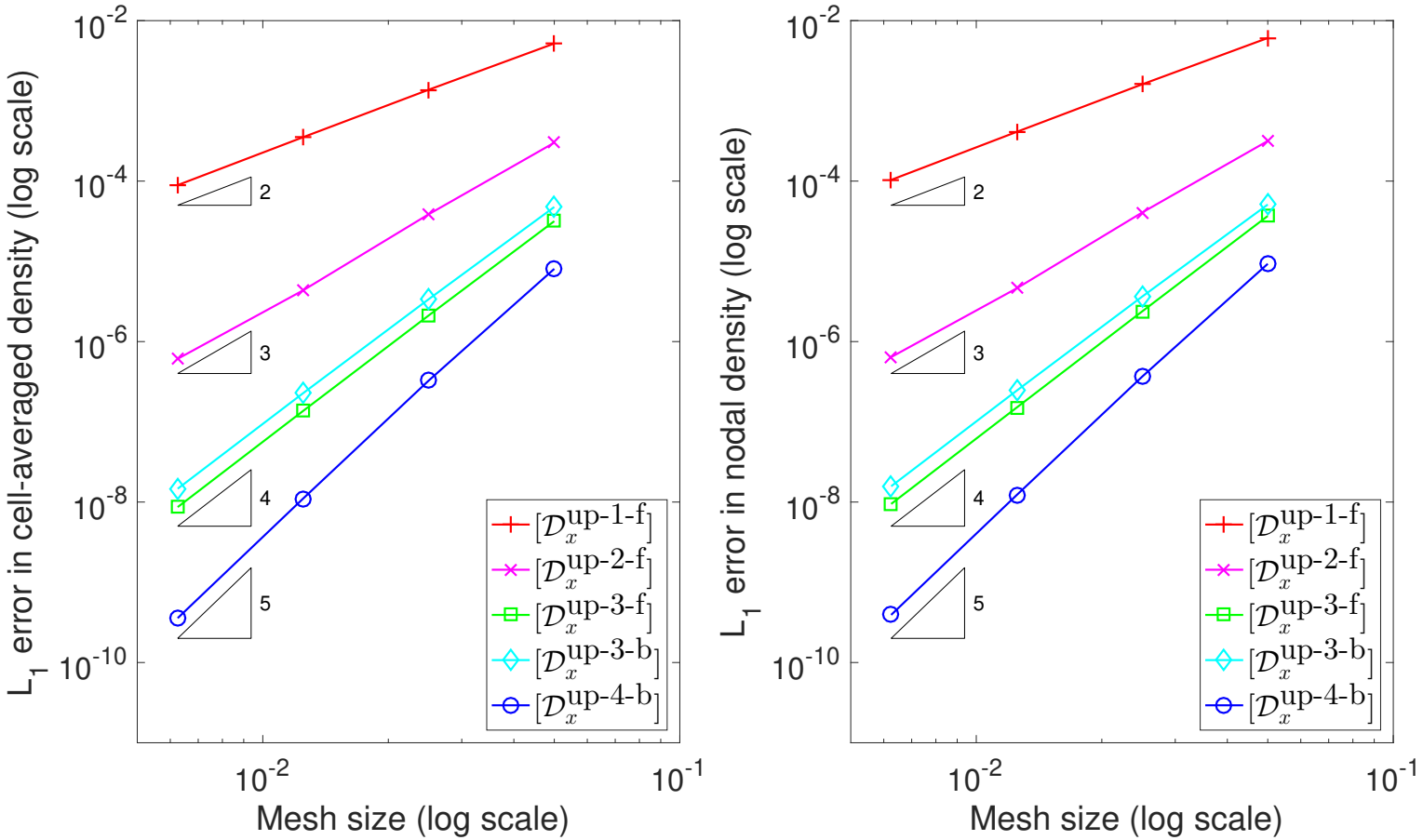

One-Dimensional Problems

Euler equations – Sod's shock tube

- Two different states are separated by a membrane that is located at $x = 0.0$ and removed at $t = 0.0$.

$$\begin{cases} \rho(x,0) = 1.0 \\ u(x,0) = 0.0\,, \quad x \in [-2,\ 0] \\ p(x,0) = 1.0 \end{cases} \quad ; \quad \begin{cases} \rho(x,0) = 0.125 \\ u(x,0) = 0.0\,, \quad x \in [0,\ 2] \\ p(x,0) = 0.1 \end{cases} \quad .$$

- The solution is composed of a left-going rarefaction and a right-going shock.
- All five HV methods using a uniform grid with 80 cells.
- Comparison to the monotone high-resolution MUSCL method with Roe flux for Euler equations and van Leer limiter.

One-Dimensional Problems

Euler equations – Sod's shock tube

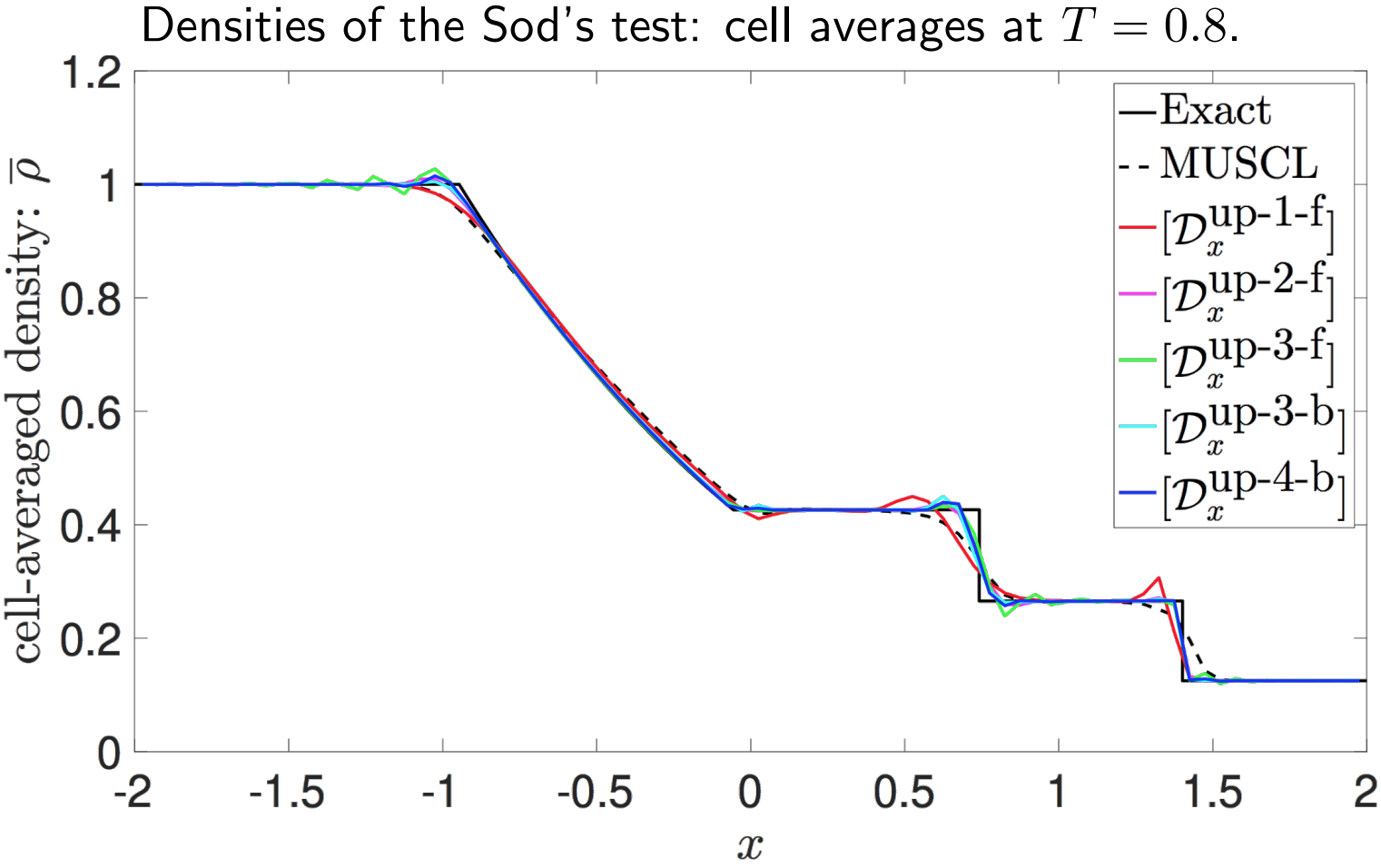

One-Dimensional Problems

Euler equations – Sod's shock tube

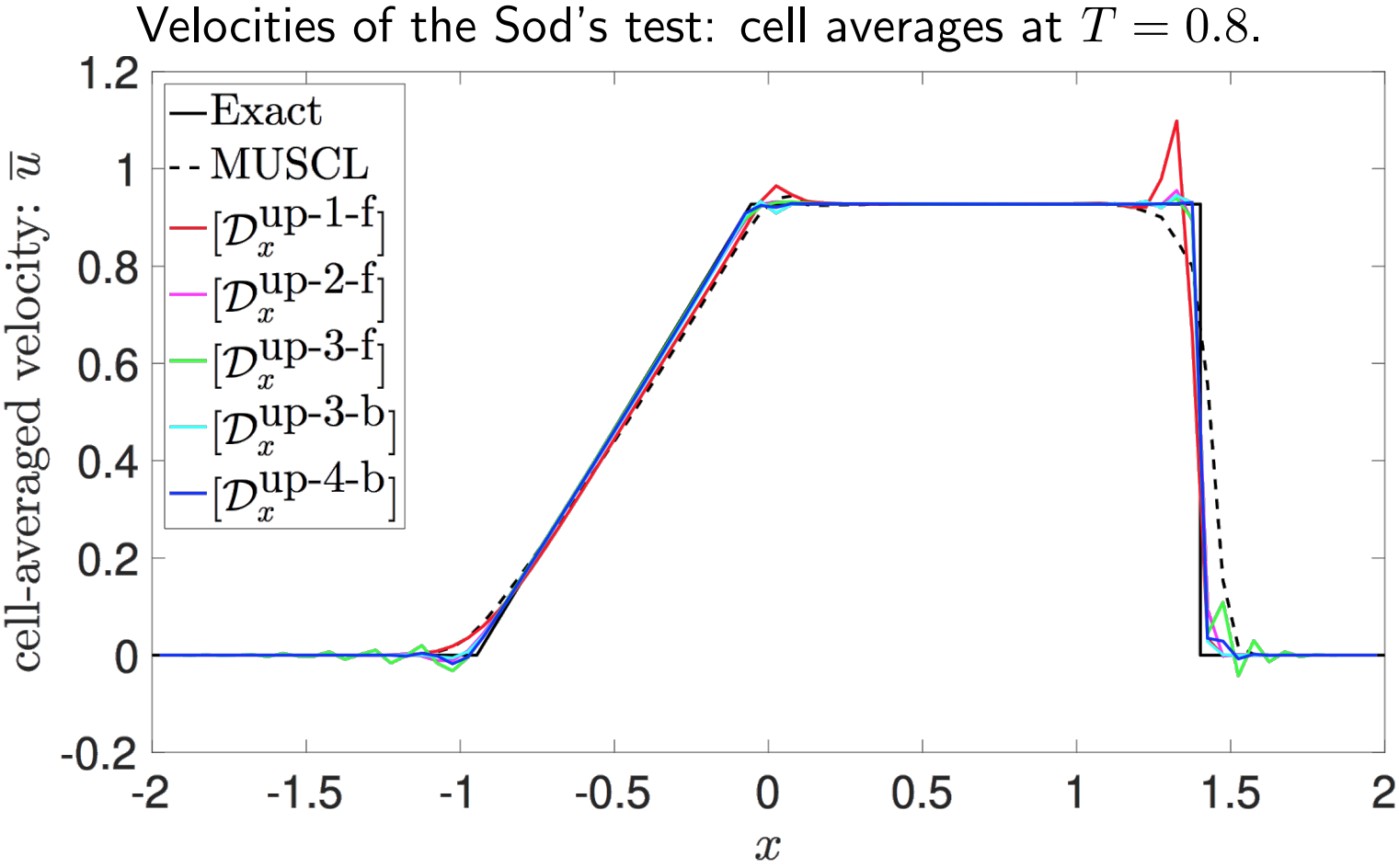

One-Dimensional Problems

Euler equations – Sod's shock tube

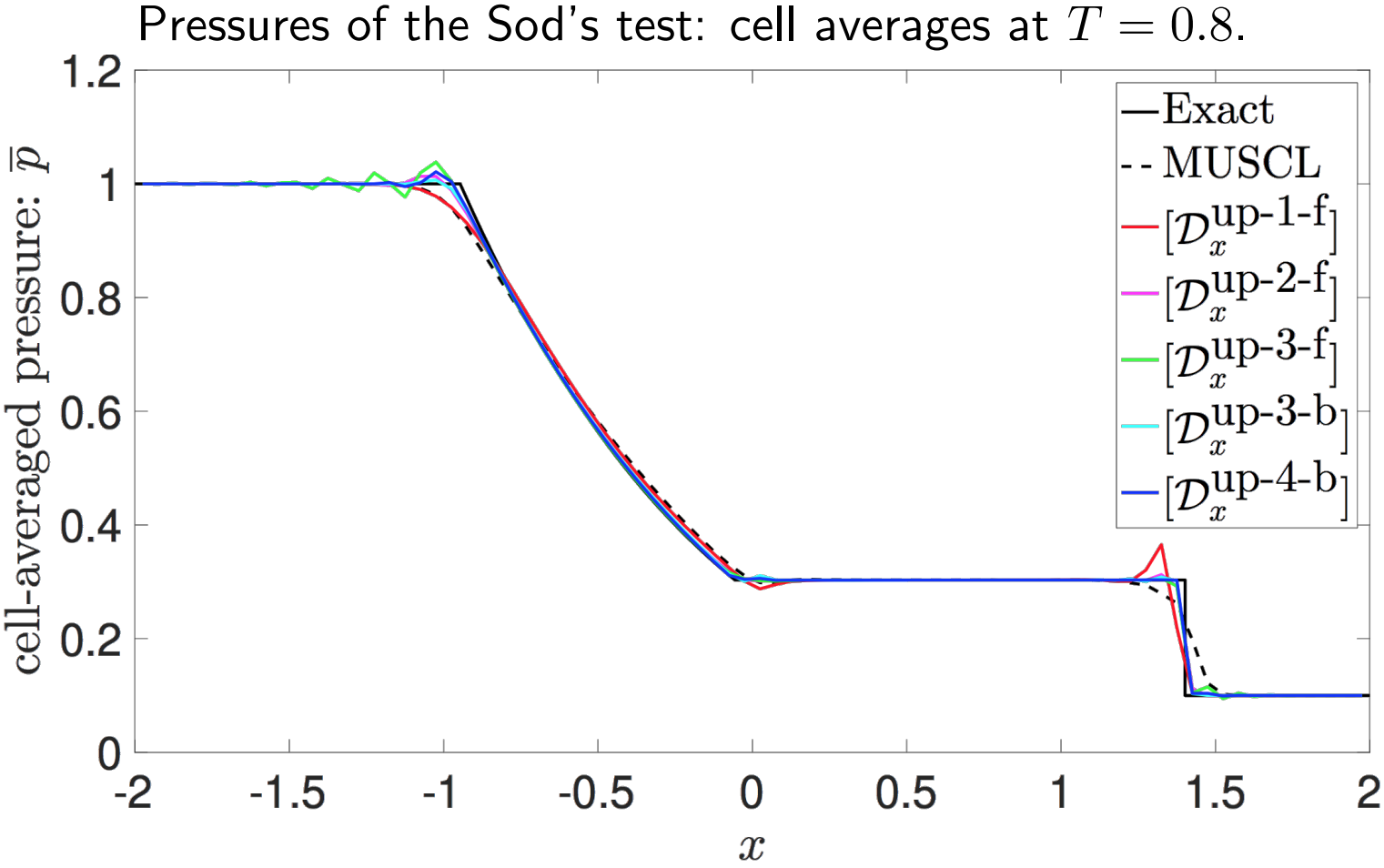

One-Dimensional Problems

Buckley-Leverett equation – double Riemann problem

- Non-convex flux function, a model problem for porous-media flows:

$$w_t + \left(\frac{4w^2}{4w^2 + (1-w)^2} \right)_x = 0 \, .$$

- Initial data is composed of two Riemann problems:

$$w(x,0) = \begin{cases} 0.1 \, , & -0.5 \leq x \leq 0.0 \\ 0.5 \, , & 0.0 < x \leq 1.0 \\ 0.2 \, , & 1.0 < x \leq 2.5 \, . \end{cases}$$

- Both Riemann solutions consist of a rarefaction connected to a shock at $f''(w_0) = 0$, where $f(w)$ is the flux function.
- All five HV methods using a uniform grid with 150 cells.

One-Dimensional Problems

Buckley-Leverett equation – double Riemann problem

Solution of the Buckley-Leverett problem: cell averages at $T = 0.4$.

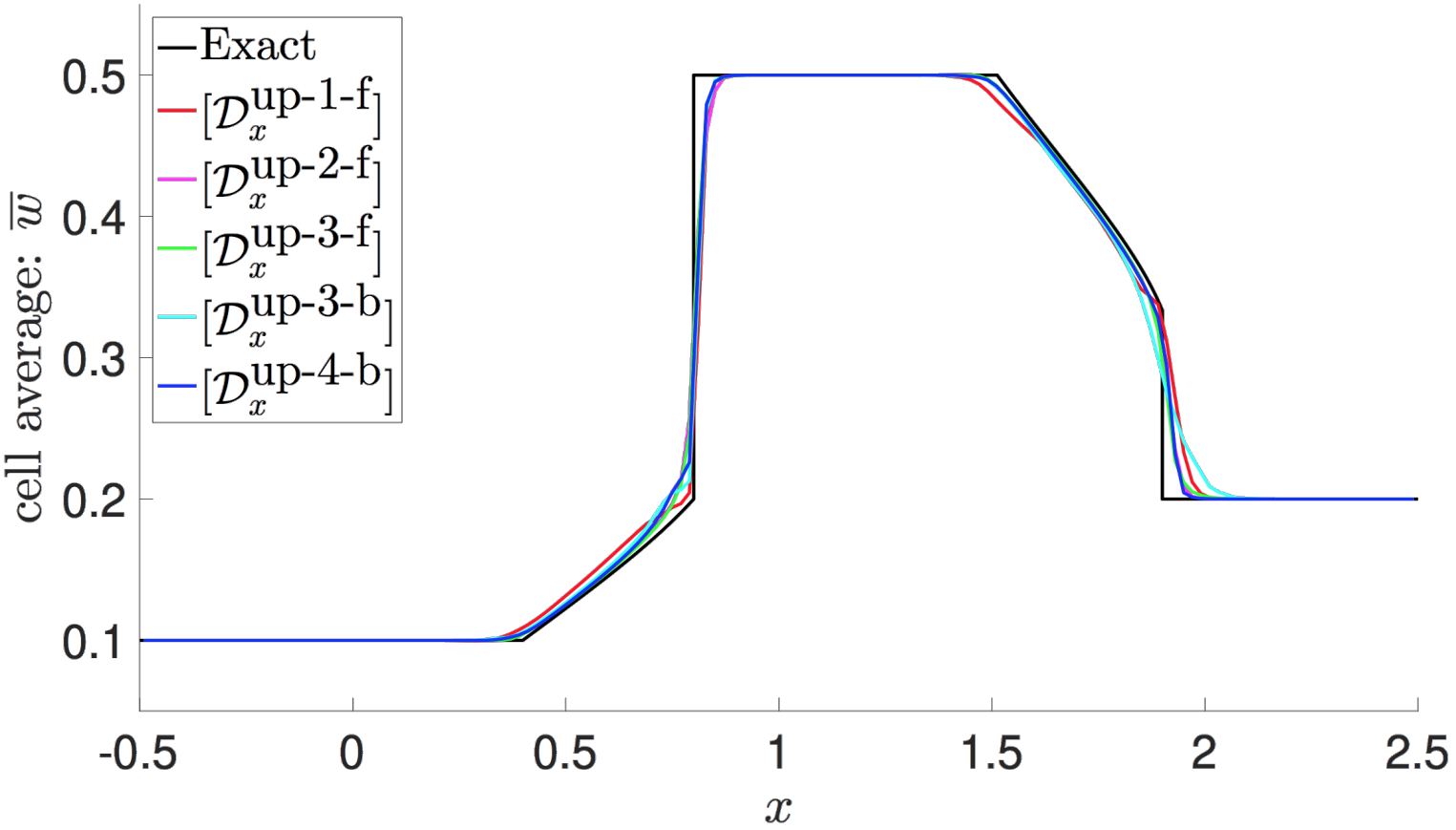

One-Dimensional Problems

Buckley-Leverett equation – double Riemann problem

Solution of the Buckley-Leverett problem: nodal values at $T = 0.4$.

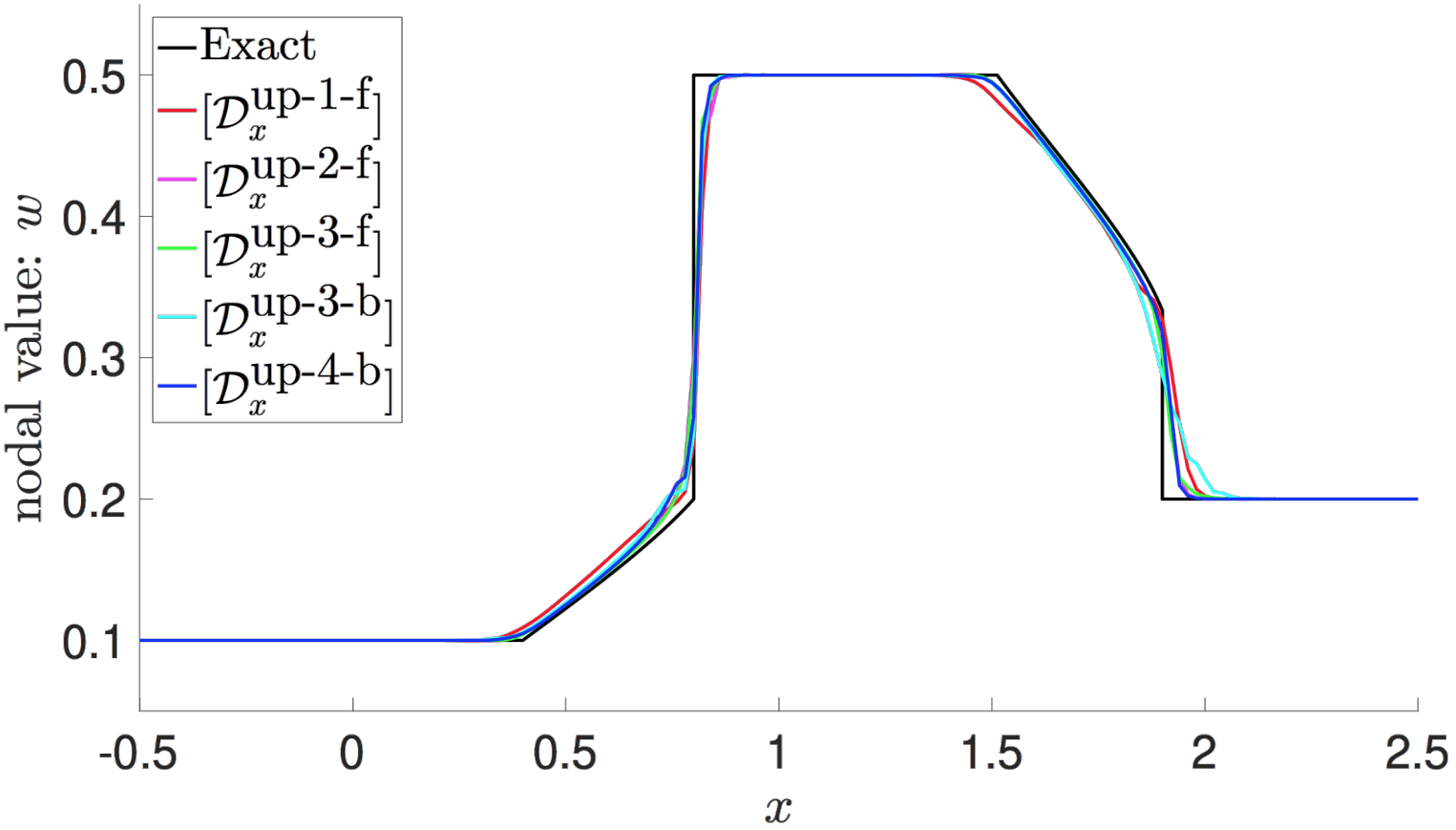

Two-Dimensional Problems

Linear advection equation (Cauchy problem)

- Cauchy problem:

$$\begin{cases} w_t + w_x + 2w_y = 0\ , & (x, y, t) \in [-1,\ 1]^2 \times [0,\ 2] \\ w(x, y, 0) = (1 + \sin(\pi\ x))(1 + \sin(2\pi\ y))\ , & (x, y) \in [-1,\ 1]^2 \\ w(-1, y, t) = w(1, y, t)\ , & y \in [-1,\ 1],\ t \in [0,\ 2] \\ w(x, -1, t) = w(x, 1, t)\ , & x \in [-1,\ 1],\ t \in [0,\ 2]\ . \end{cases}$$

- Exact solution at $T = 2$ overlaps with the initial data.
- The two HV methods as well as an unlimited second-order FVM.
- Comparison to the high-resolution MUSCL method with Rusanov flux and no limiter.
- A sequence of four uniform grids: 40×40, 80×80, 160×160, and 320×320.

Two-Dimensional Problems

Linear advection equation (Cauchy problem)

L_1-errors in cell averages (left) and nodal values (right) in logarithmic scales.

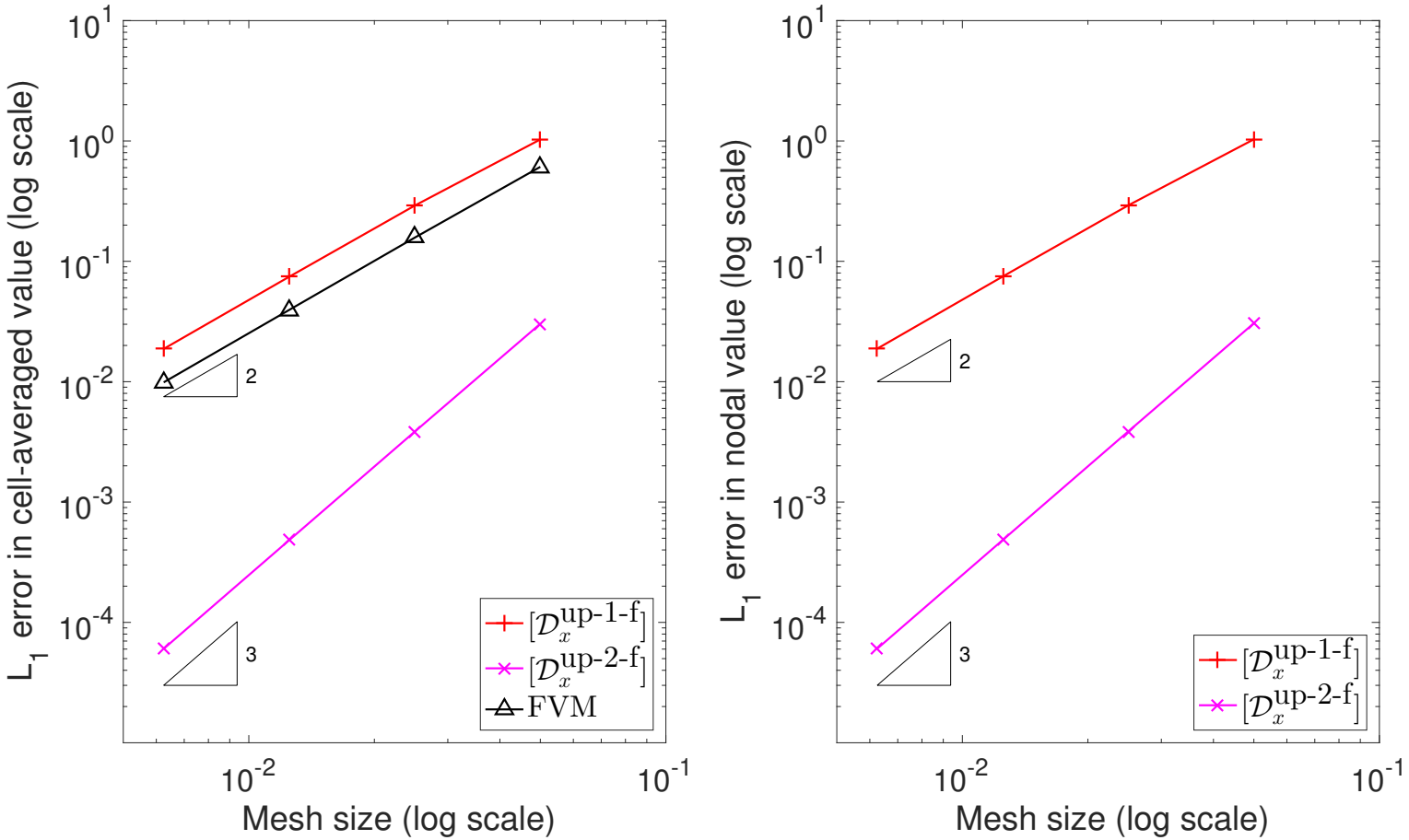

Two-Dimensional Problems

Linear advection equation (Cauchy problem)

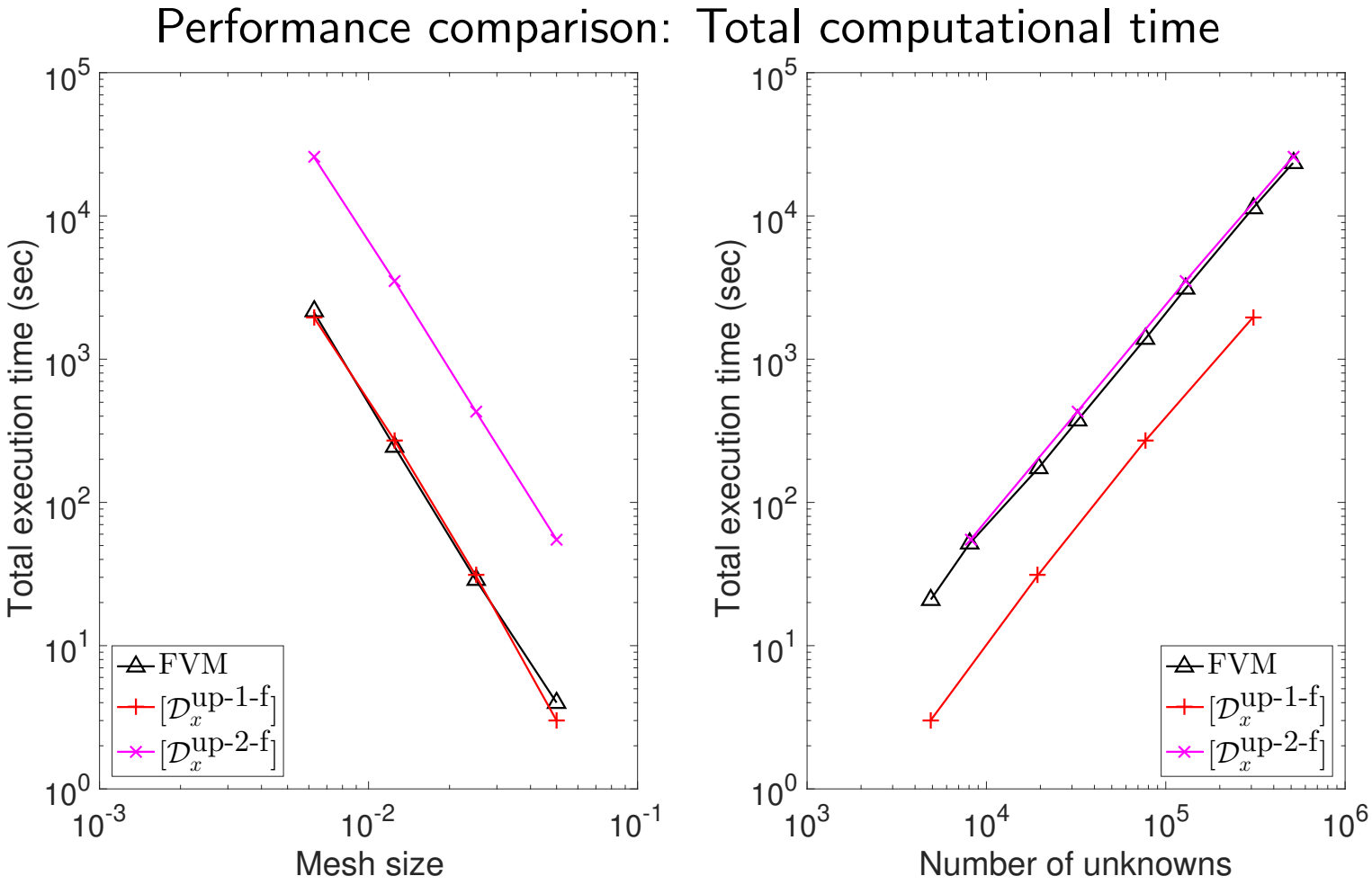

Two-Dimensional Problems

Linear advection equation (Cauchy problem)

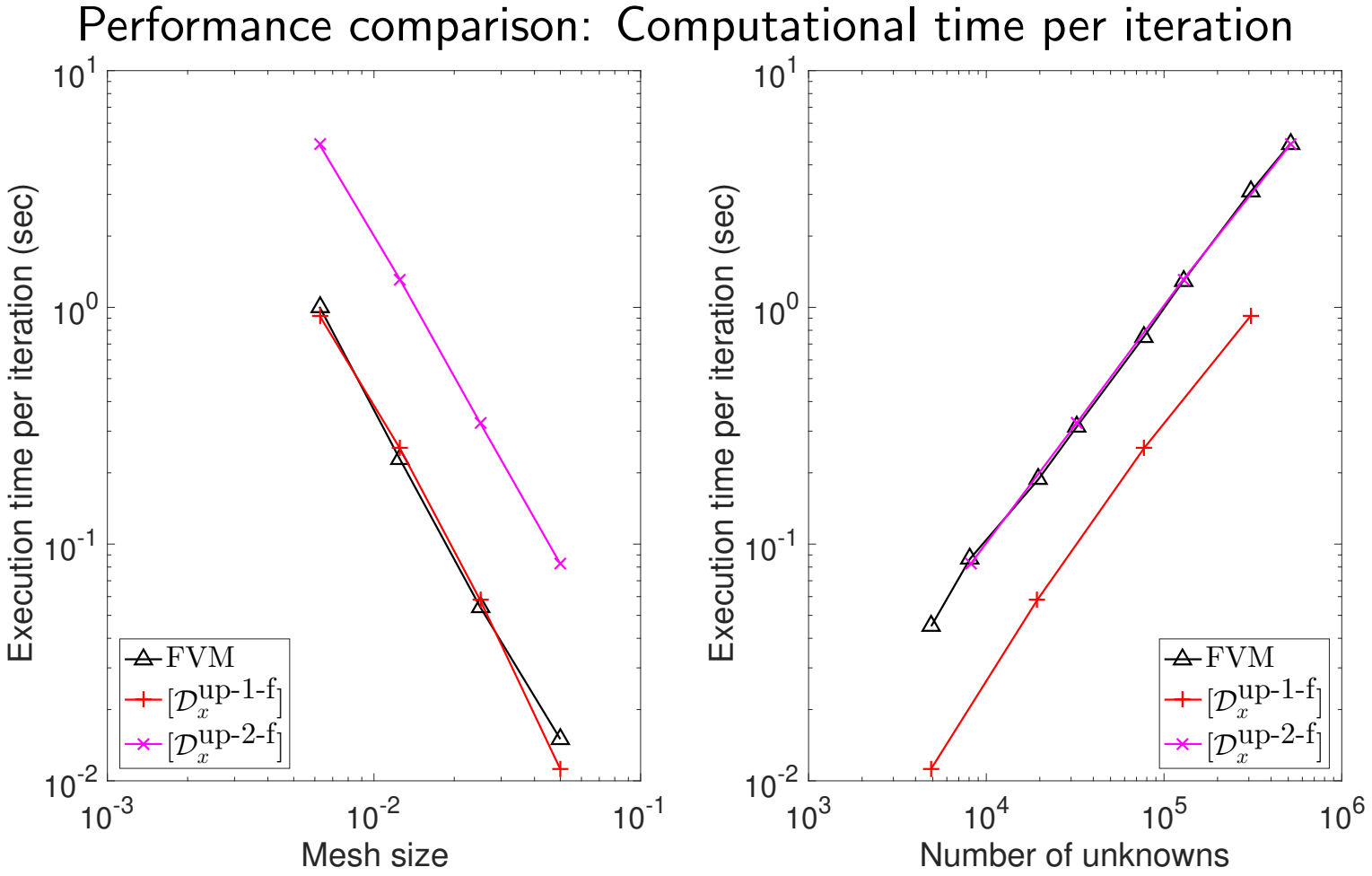

Two-Dimensional Problems

Linear advection equation (Cauchy problem)

Performance comparison: Computational time per iteration per unknown

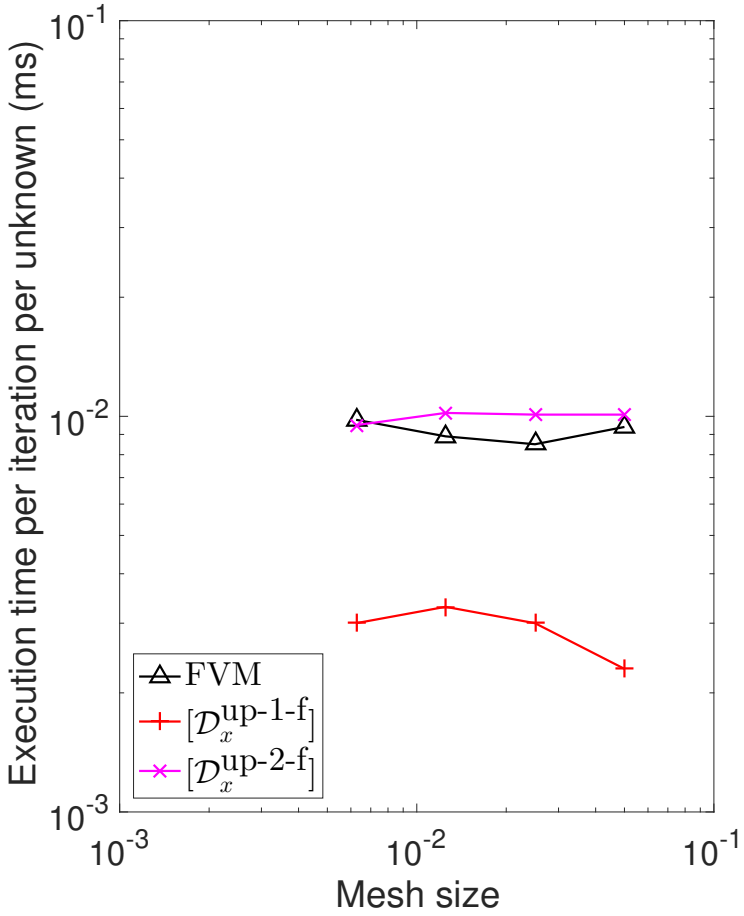

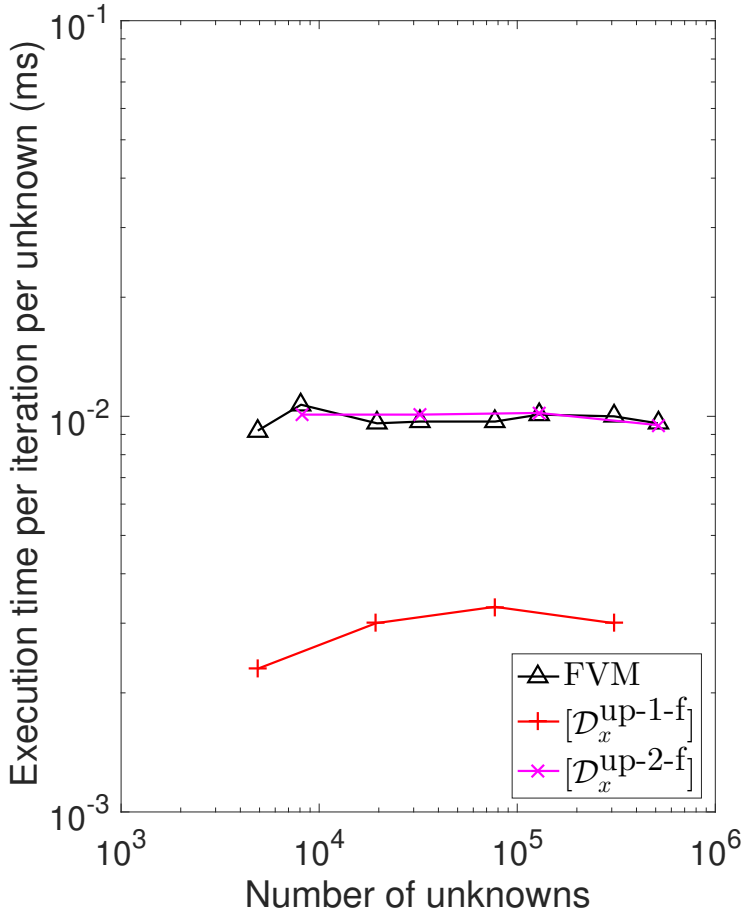

Two-Dimensional Problems

Isentropic vortex advection

- Two-dimensional Euler equations.
- Initial data represents a isentropic vortex on a periodic domain $[-5,\ 5]^2$:

$$\begin{cases} \rho(x,y,0) = \left(1 - \frac{(\gamma-1)\epsilon^2}{8\gamma\pi^2}\exp\left(1-x^2-y^2\right)\right)^{\frac{1}{\gamma-1}} \\ u(x,y,0) = 1 - \frac{\epsilon y}{2\pi}\exp\left(\frac{1}{2}(1-x^2-y^2)\right) \\ v(x,y,0) = 1 + \frac{\epsilon x}{2\pi}\exp\left(\frac{1}{2}(1-x^2-y^2)\right) \\ p(x,y,0) = \left(1 - \frac{(\gamma-1)\epsilon^2}{8\gamma\pi^2}\exp\left(1-x^2-y^2\right)\right)^{\frac{\gamma}{\gamma-1}} \end{cases},$$

  where $\gamma = 1.4$ and $\epsilon = 5.0$.
- The vortex advects with velocity $(1, 1)$.
- The two HV methods as well as an unlimited second-order FVM.
- A sequence of four uniform grids: 40×40, 80×80, 160×160, and 320×320.

Two-Dimensional Problems

Isentropic vortex advection

L_1-errors in $\overline{\rho}$ (left) and ρ (right) in logarithmic scales.

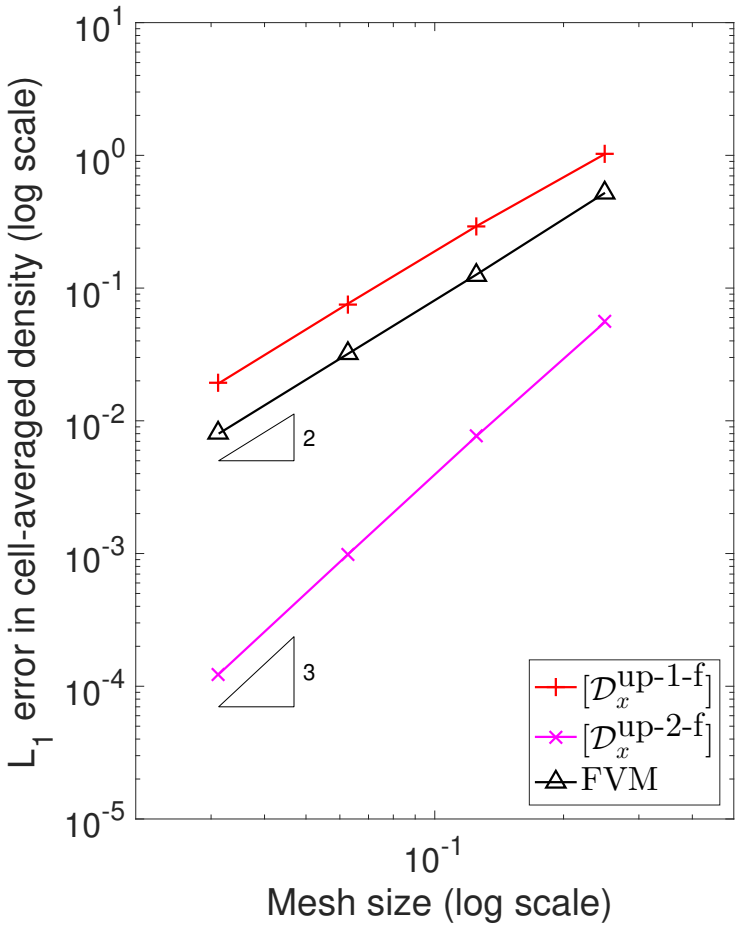

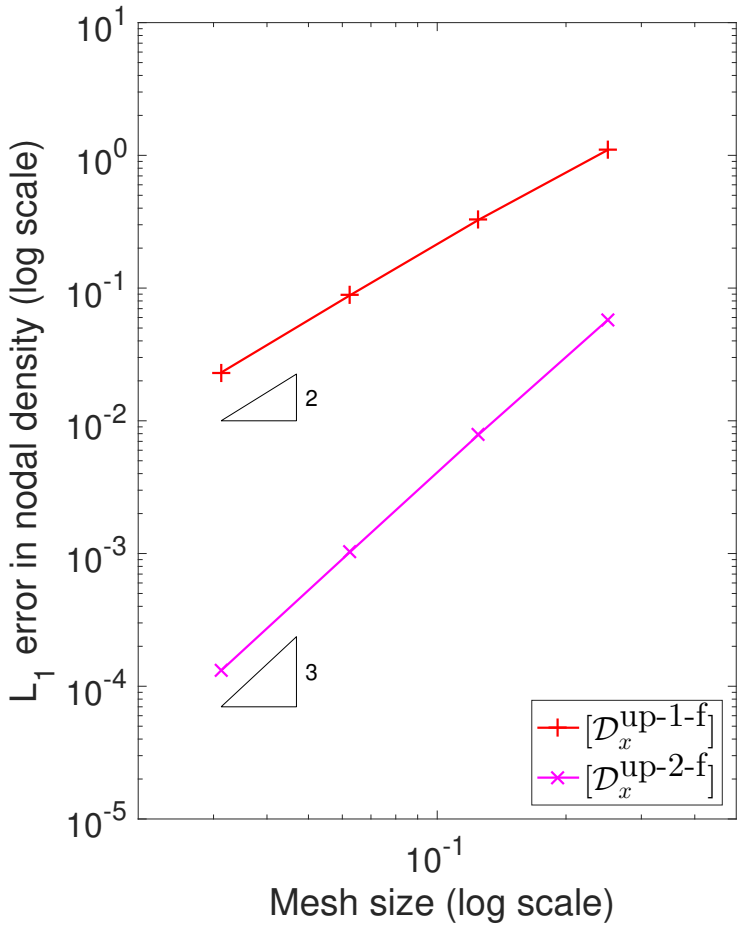

Two-Dimensional Problems

Isentropic vortex advection

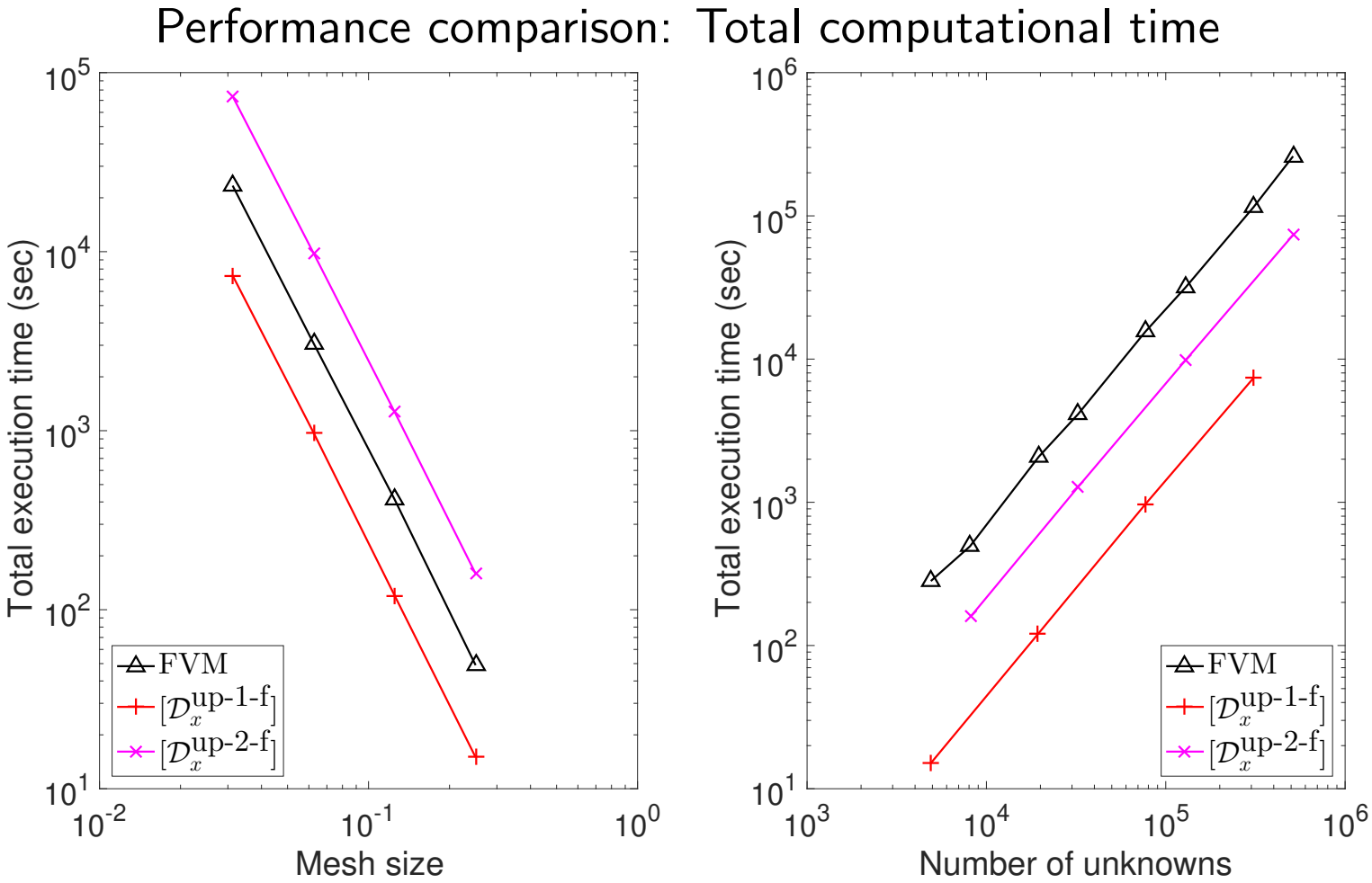

Two-Dimensional Problems

Isentropic vortex advection

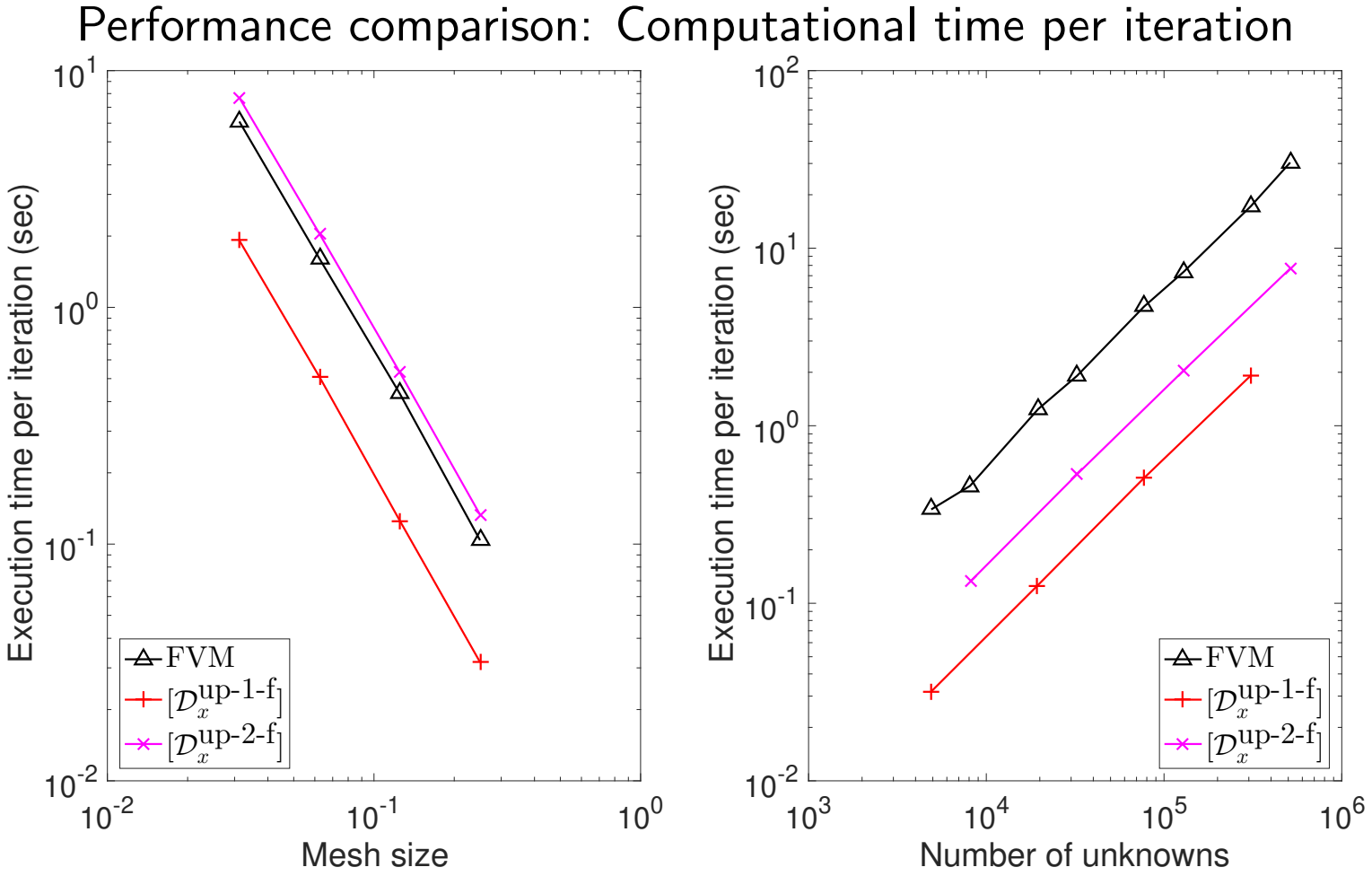

Two-Dimensional Problems

Isentropic vortex advection

Performance comparison: Computational time per iteration per unknown

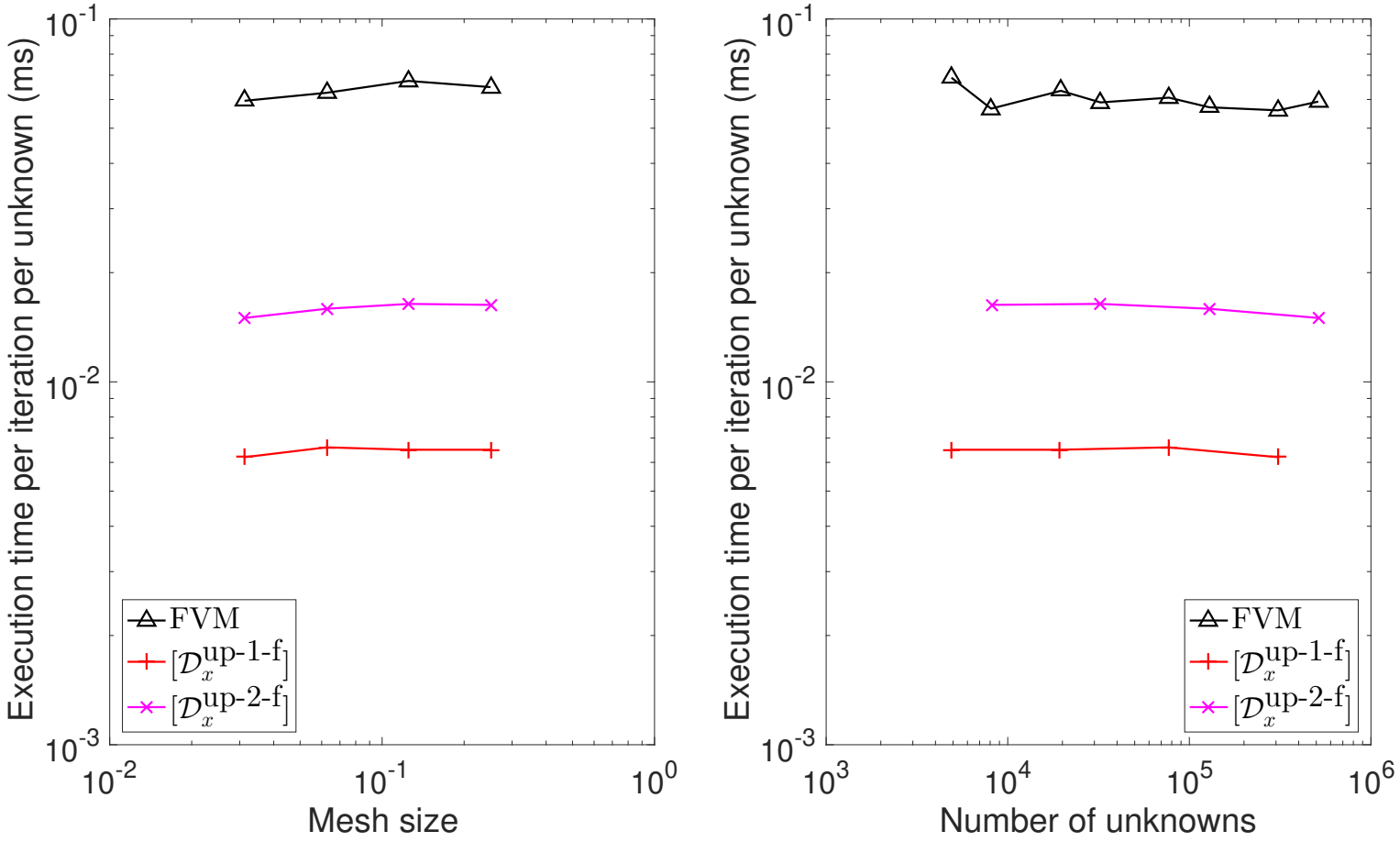

Conclusions and Future Directions

Conclusions

We present a hybrid-variable (HV) approach for advection equations:

- Construct HV-DDO of arbitrary order of accuracy explicitly.
- Prove superior accuracy.
- Generalize the upwind condition.
- A systematic procedure to verify the linear stability.
- Extensions to nonlinear systems and higher dimensions.

Conclusions and Future Directions

Conclusions

We present a hybrid-variable (HV) approach for advection equations:

- Construct HV-DDO of arbitrary order of accuracy explicitly.
- Prove superior accuracy.
- Generalize the upwind condition.
- A systematic procedure to verify the linear stability.
- Extensions to nonlinear systems and higher dimensions.

Future directions

- Refine the order star analysis to prove tighter barrier.
- Construct all linearly stable HV methods.
- Nonlinear stability enhancement (such as L_1-stability).
- Entropy inequality.